of infected cells through activation of the ATR-mediated DNA damage response. PLoS Pathog. 5 (10), e1000613.

Weil, A.F., Ghosh, D., Zhou, Y., Seiple, L., McMahon, M.A., Spivak, A.M., Siliciano, R.F., Stivers, J.T., 2013. Uracil DNA glycosylase initiates degradation of HIV-1 cDNA containing misincorporated dUTP and prevents viral integration. Proc. Natl. Acad. Sci. U.S.A. 110 (6), E448–E457.

Wen, X.Y., Klockow, L.C., Nekorchuk, M., Sharifi, H.J., de Noronha, C.M.C., 2012. The HIV1 protein Vpr acts to enhance constitutive DCAF1-dependent UNG2 turnover. PLoS One 7 (1), e30939.

Xu, H.Z., Chertova, E., Chen, J.B., Ott, D.E., Roser, J.D., Hu, W.S., Pathak, V.K., 2007. Stoichiometry of the antiviral protein APOBEC3G in HIV-1 virions. Virology 360 (2), 247–256.

Yan, N., O'Day, E., Wheeler, L.A., Engelman, A., Lieberman, J., 2011. HIV DNA is heavily uracilated, which protects it from autointegration. Proc. Natl. Acad. Sci. U.S.A. 108 (22), 9244–9249.

Yang, B., Chen, K.Y., Zhang, C., Huang, S., Zhang, H., 2007. Virion-associated uracil DNA glycosylase-2 and apurinic/apyrimidinic endonuclease are involved in the degradation of APOBEC3G-edited nascent HIV-1 DNA. J. Biol. Chem. 282 (16), 11667–11675.

Yu, X.H., Yu, Y.K., Liu, B.D., Luo, K., Kong, W., Mao, P.Y., Yu, X.F., 2003. Induction of APOBEC3G ubiquitination and degradation by an HIV-1 Vif-Cul5-SCF complex. Science 302 (5647), 1056–1060.

Zhao, R.Y., Li, G., Bukrinsky, M.I., 2011. Vpr-host interactions during HIV-1 viral life cycle. J. Neuroimmune Pharmacol. 6 (2), 216–229.

Zheng, Y.H., Irwin, D., Kurosu, T., Tokunaga, K., Sata, T., Peterlin, B.M., 2004. Human APOBEC3F is another host factor that blocks human immunodeficiency virus type 1 replication. J. Virol. 78 (11), 6073–6076.

SCIENTIFIC REPORTS

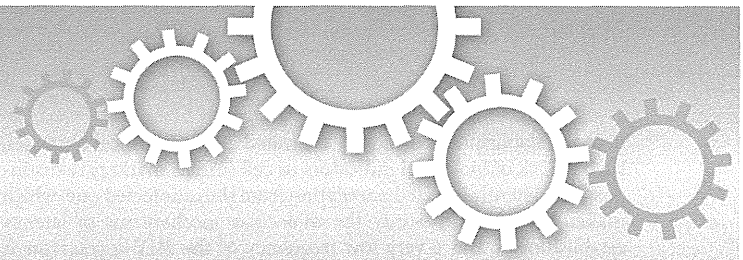

OPEN

SUBJECT AREAS:
VIROLOGY
EPIGENETICS

Received
3 February 2014

Accepted
8 December 2014

Published
9 January 2015

Correspondence and requests for materials should be addressed to T.W. (tnabe@ims.u-tokyo.ac.jp) or M.Y. (myamagishi@mgs.k.u-tokyo.ac.jp)

Epigenetic Heterogeneity in HIV-1 Latency Establishment

Yuka Matsuda[1], Mie Kobayashi-Ishihara[2], Dai Fujikawa[1], Takaomi Ishida[3], Toshiki Watanabe[1] & Makoto Yamagishi[1]

[1]Laboratory of Tumor Cell Biology, Department of Medical Genome Sciences, Graduate School of Frontier Sciences, The University of Tokyo, 4-6-1 Shirokanedai, Minato-ku, Tokyo 108-8639, Japan, [2]Department of Immunology, National Institute of Infectious Diseases, 1-23-1 Toyama, Shinjuku-ku, Tokyo 162-8640, Japan, [3]Research Center for Asian Infectious Disease, Institute of Medical Science, The University of Tokyo, 4-6-1 Shirokanedai, Minato-ku, Tokyo 108-8639, Japan.

Despite prolonged antiretroviral therapy, HIV-1 persists as transcriptionally inactive proviruses. The HIV-1 latency remains a principal obstacle in curing AIDS. It is important to understand mechanisms by which HIV-1 latency is established to make the latent reservoir smaller. We present a molecular characterization of distinct populations at an early phase of infection. We developed an original dual-color reporter virus to monitor LTR kinetics from establishment to maintenance stage. We found that there are two ways of latency establishment i.e., by immediate silencing and slow inactivation from active infection. Histone covalent modifications, particularly polycomb repressive complex 2 (PRC2)-mediated H3K27 trimethylation, appeared to dominate viral transcription at the early phase. PRC2 also contributes to time-dependent LTR dormancy in the chronic phase of the infection. Significant differences in sensitivity against several stimuli were observed between these two distinct populations. These results will expand our understanding of heterogeneous establishment of HIV-1 latency populations.

Human immunodeficiency virus type 1 (HIV-1) is a causative agent of acquired immunodeficiency syndrome (AIDS). After the discovery of HIV-1, five classes of antiretroviral drugs have been developed and a combination of antiretroviral drug treatment (ART) effectively prevents viral replication under the detectable limit[1,2]. However, the infected individuals should continue the ART for life because interruption in the ART results in a rapid viral rebound[3–5]. Despite prolonged ART, HIV-1 persists as a transcriptionally inactive provirus in some cell types and at anatomical sites, which is defined as a HIV-1 latent reservoir[6]. This virus reservoir is now a major obstacle for HIV-1 cure, because the ART alone cannot eradicate this population. Interestingly, detailed studies of residual viremia have shown that the rebound virus is archival and non-evolving from the virus before ART[7–9]. Latently infected CD4 T cells harboring competent provirus are thought to be a major source of intact HIV-1.

The HIV-1 5′LTR, located at the 5′ end of the integrated provirus, contains the promoter and enhancer elements that accelerate HIV-1 transcription by host transcription factors, including NF-κB, NFAT, and Sp1[10–12]. The HIV-1-encoded regulatory protein Tat is necessary for sufficient viral transcription initiation and elongation[13,14]. In contrast, the integrated provirus forms a nucleosome structure that is affected by epigenetic regulation such as histone modification and DNA methylation. The regulators of histone acetylation and methylation negatively control HIV-1 transcription, leading to transcriptional latency[15–18].

HIV-1 transcription is frequently silenced by epigenetic changes in the residual reservoir under ART[6]. Reversing latency has been proposed to eliminate latently infected cells[19]. Several activation strategies combined with the ART have been attempted, including cytokine-based immune activation therapy using interleuin-2 (IL-2) or interferon-γ (IFN-γ) and prescriptions of epigenetic drugs[20–24]. In particular, inhibitors of epigenetic factors are respected as reagents to reactivate viruses in a large spectrum of reservoirs without inducing cell activation or proliferation. Recent clinical trials revealed that histone deacetylase (HDAC) inhibitors, valproic acid (VPA) and vorinostat (SAHA) could reactivate plasma viral RNA level in patients undergoing long-term ART[25,26].

Much attention has been paid to define how the viral latency is maintained and how the latent viruses can be effectively reactivated. By using some latent models, many researchers have reported the molecular mechanisms contributing to the maintenance of viral gene suppression, including the host epigenetic system, Tat mutation, sequence variation in the LTR, and depletion of elongation factors[27]. It is important to understand the mechanisms by which HIV-1 latency is established to make the latent reservoir size smaller. However, detailed informa-

tion on establishment of latency is limited due to technical obstacles, such as lack of biological indicators or cell surface markers to distinguish the latently infected population from the uninfected one, which makes it difficult to study the molecular mechanisms of latency establishment, and a very low frequency of the HIV-1 reservoir is estimated in actually infected individuals[28]. The most difficult problem is that the small reservoir population possesses the capability to cause immunodeficiency again.

In the present study, we developed an original reporter virus, enabling us to dissect the infected and uninfected populations and to monitor the LTR kinetics from establishment to maintenance step. We found two modes of infection, the immediately silenced and active infections. We also identified the molecular underpinnings of HIV-1 silencing by comparing the two distinct populations. Histone methylation, particularly polycomb repressive complex 2 (PRC2)-mediated histone H3 lysine 27 (H3K27) trimethylation, appears to affect viral transcription at the early phase of infection. In addition, PRC2 also contributes to the time-dependent repression of LTR activity in the actively infected population. These two distinct populations showed differential responses to physiological and pharmacological stimulations. Intervention of epigenetic regulation by multi-targeting of histone modifiers resulted in restoring the LTR activity in both populations.

Results

Establishment of a new HIV-1 silencing model. To evaluate the dynamics of LTR activity at the early phase of HIV-1 infection, we developed an original lentivirus vector that carries the double reporter genes, LTR–*Tat*–IRES–*Venus*–EF1α–*mRFP* (Fig. 1a). This reporter construct contains two different genes encoding fluorescent proteins, Venus and mRFP, whose expressions are controlled by the HIV-1 LTR sequence and EF1α promoter, respectively. EF1α promoter activity is stable, supporting that mRFP expression can be used as an infected cell indicator (Supplementary Fig. 1a). In addition, this virus doesn't show any cytotoxicity because of the absence of viral genes except *tat*. We first transiently introduced the plasmids, CS–LTR–*Tat*–IRES–*Venus*–EF1α–*mRFP* and CS–LTR–empty–IRES–*Venus*–EF1α–*mRFP*, into 293FT cells. The expression levels of the two fluorescent proteins could be simultaneously monitored by flow cytometric analysis (Fig. 1b). Compared with the *Tat*(−) vector, the *Tat*(+) vector induced high Venus expression, indicating that this reporter represented *in vivo* LTR action. Promoter interference appeared to be a little because the Venus level was directly proportional to mRFP expression.

Following this, we produced a VSV-G pseudotyped single-round reporter virus solution and transduced it in the Jurkat human T cell line to continuously evaluate the LTR activity after proviral integration into the host genome. The LTR activity within infected cells was defined by sequential gating beginning with FSC/SSC to select intact lymphocytes, subgating on the mRFP(+) and/or Venus(+) population, and calculating the Venus profile (Fig. 1c). Venus expression was detected in cells with LTR–*Tat*–IRES–*Venus*–EF1α–*mRFP* virus compared with cells with *Tat*(−) reporter virus at 3 days post-infection (dpi), suggesting that the LTR activity was immediately silenced when cell lacked the Tat protein. The mean of LTR activity reached a peak 4 dpi and the LTR activity and Venus(+) population size gradually decreased during prolonged cultivation (Fig. 1d). We confirmed using a single-color reporter (CS–LTR–*tat*–IRES–*Venus*) that the loss of LTR activity was not due to the effect of downstream EF1α promoter DNA (Supplementary Figs. 1b–d). The LTR activity was substantially silenced at 40 dpi. We treated this population with PMA/Ionomycin or TNF-α as NF-κB activators and detected robust Venus expression, indicating that the decrease in Venus level was caused by LTR inactivation (Fig. 1e). In addition, treatment with VPA restored the LTR activity in a dose-dependent manner, resembling the latently infected HIV-1 in ART-treated individuals[29] (Fig. 1f). Thus, these data demonstrated that the new reporter system could represent the physiological silencing of HIV-1 transcription. We note that a part of infected cells remained as Venus(−).

Two modes of latency establishment. We observed the establishment of HIV-1 infection in various cells. The human T cell lines, CCRF-CEM, SupT1, and Jurkat cells and HEK293FT cells were infected with the LTR–*Tat*–IRES–*Venus*–EF1α–*mRFP* virus and analyzed for Venus expression within the infected population [Venus(+) and/or mRNP(+)] at 3 dpi. We found that two major populations emerged in all the tested cell lines, one had strong Venus expression and the other showed weak or no Venus expression (Figs. 1c and 2a). Further, we examined the LTR activity in human CD4 T cells, primary host cells of latency, by using the highly concentrated dual-color reporter, which allowed us to analyze the LTR activity without the viral protein-dependent cytotoxicity. Spinoculation method facilitated viral entry and following integration in non-dividing primary cells. Resting CD4+ T cells from a healthy donor were infected with the reporter, and the Venus expression within the infected population was evaluated at 3 dpi, which is an early phase of HIV-1 infection. We found substantial population of cells expressing the latency-associated fluorescent marker (Venus(−)/mRFP(+)) in primary CD4+ T cells (Fig. 2b). T cell activation by anti-CD3/CD28 antibodies reduced the latently infected population.

To further characterize the distinct populations, we sorted the infected Jurkat cells by Venus/mRFP fluorescences. Each population could be sorted with a cell sorter system at 3 dpi and was subjected to the following analyses (Fig. 3a): First, Alu-PCR analysis of genomic DNA detected similar amount of proviral DNA either in the actively or silently infected populations (Fig. 3b). Absolute quantification of *Venus* mRNA level demonstrated that the Venus expression pattern appeared varied due to the transcriptional activity of LTR (Fig. 3c). Indeed, transcriptional stimulation by PMA/Ionomycin or TNF-α treatment partially restored the LTR activity and *Venus* mRNA in the silent integration population (Fig. 3d).

According to previous literatures, we investigated the epigenetic status of both integrated LTR in the above sample set. HIV-1 LTR contains some CpG sites that contribute to transcriptional repression[30,31]. However, bisulfate DNA sequencing showed no acquisition of CpG methylation at LTR in either population (data not shown). Whereas, evaluation of covalent histone modifications by ChIP assay revealed that histone H3 acetylation (H3Ac) and H3K4 trimethylation (H3K4me3), which were active histone markers, were specifically gained at the LTR region within the Venus(+) population (Fig. 3e). In contrast, histone H3K27 trimethylation (H3K27me3), which was a general repressive histone marker, was specifically accumulated at the promoter region of LTR in the Venus(−) population (Fig. 3e). Another repressive histone mark H3K9 trimethylation (H3K9me3), which has been implicated in HIV-1 latency, was not different between the two populations. To further address the LTR silencer during immediate latency establishment, we focused on levels of the H3K27me3 marker and its specific methyltransferase complex, polycomb repressive complex 2 (PRC2). ChIP assay revealed selective occupancies of EZH2 and SUZ12, essential components of PRC2, at the LTR region within the Venus(−) population (Fig. 3f). Inhibition of PRC2 by treatment with DZNep, an inhibitor of EZH2 that was an PRC2 catalytic unit, partially reactivated the LTR activity in a dose-dependent manner, demonstrating participation of PRC2 in the immediate silencing of LTR (Fig. 3g). Of note, co-treatment with DZNep and VPA or SAHA resulted in more effective LTR transactivation, suggesting that HDACs and PRC2 cooperate in the establishment of silent integration of HIV-1. Indeed, CTD-phosphorylated Pol II occupancy in LTR region was enhanced when PRC2 and HDAC were simultaneously inhibited (Fig. 3h).

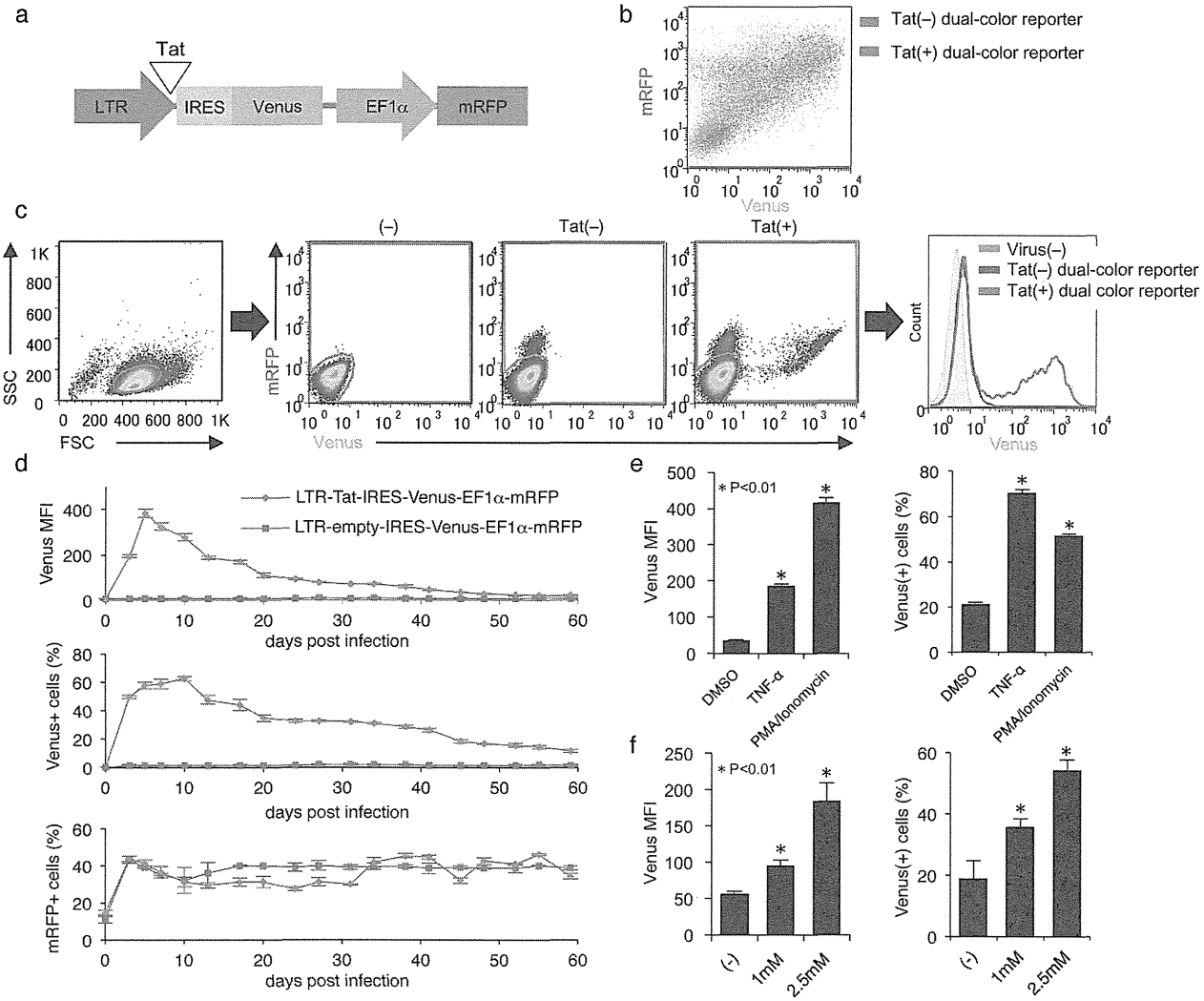

Figure 1 | Establishment of new HIV-1 silencing model. (a) Construction of dual-color reporter lentivirus. Venus and mRFP expressions are controlled by LTR and EF1α promoter, respectively. *Tat* was inserted downstream of the LTR sequence. (b) HEK293FT cells were transiently transfected with the CS–LTR–*Tat*–IRES–*Venus*–EF1α–*mRFP* or CS–LTR–empty–IRES–*Venus*–EF1α–*mRFP* plasmid. The expression levels of the fluorescent proteins at 2 days post transfection were analyzed by flow cytometry. (c) Jurkat T cell line was infected with the CS–LTR–*Tat*–IRES–*Venus*–EF1α–*mRFP* or CS–LTR–empty–IRES–*Venus*–EF1α–*mRFP* lentivirus. The LTR activity within infected population was defined by sequential gating beginning with FSC/SSC to select intact lymphocytes (left scatter plot), subgating on the mRFP(+) and/or Venus(+) population (middle scatter plots). Venus expression level within the infected population was shown in histogram plots (right). (d) Kinetic analysis within the infected population (n = 3, mean ± SD). Upper graph shows kinetics of Venus mean fluorescence intensity (MFI); middle and lower show proportions of Venus(+) and mRFP(+) cells (%). (e,f) The LTR-silenced total population (48 days post infection (dpi)) were treated with TNF-α (10 ng/ml) for 16 hours or PMA (100 ng/ml)/Ionomycin (1 μM) for 24 hours (e) and VPA (indicated concentrations) for 48 hours (f). The Venus MFI (left) and Venus(+) population size (right) are shown (n = 3, mean ± SD).

Involvement of PRC2 in establishing HIV-1 latency. HIV-1 integration preferentially occurs at active chromatin sites[32,33], where transcription is dynamically regulated by PRC2-mediated chromatin conformation. The results of ChIP assay and reactivation study implicated the involvement of PRC2 in the early phase of HIV-1 transcription silencing (Fig. 3). We performed knockdown experiments using shRNAs against PRC2 components EZH2 and SUZ12 to gain mechanistic insight into the contribution of PRC2 in the induction of LTR silencing. We tested previously validated shRNA sequences and selected one shRNA that showed the highest knockdown efficiency (Fig. 4a). Durable gene suppression was achieved by retrovirus-mediated stable shRNA expression. Jurkat cells were first transduced with shRNA-expressing retrovirus to establish stable knockdown and then infected with the reporter virus (Fig. 4b–g). Flow cytometry plots with sequential gating with FSC/SSC and mRFP/Venus profiles revealed that the population size of the Venus(−) cells declined in the SUZ12- and EZH2-knockdowned or DZNep pre-treated cells (Fig. 4c–d). Alu-PCR showed almost the same amount of integrated LTR in these cells (Fig. 4e). ChIP assay also demonstrated the reduction of H3K27me3 level on LTR region in the PRC2-depleted cells, suggesting rapid accumulation of the repressive histone modification in a part of infected population (Fig. 4f). A continuous culture revealed that PRC2 depletion induced higher LTR activity at the early time point (4 dpi) and inhibited time-dependent LTR silencing (Fig. 4g). Thus, PRC2 is suggested to be involved in rapid formation of the latently infected population.

To validate these results based on the new reporter construct, we employed a single-round HIV-1, which is a more practical model of HIV-1 infection. The molecular clone pNLnGFP-Kp, in which *env*

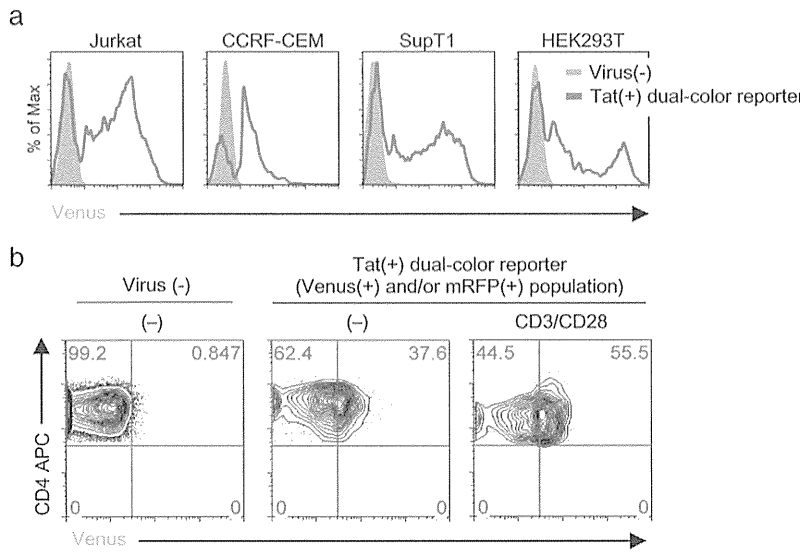

Figure 2 | LTR activity at establishment phase of HIV-1 infection. (a) Jurkat, CCRF-CEM, and SupT1 human T cell lines and HEK293T cells were infected with LTR–*Tat*–IRES–*Venus*–EF1α–*mRFP* virus. The LTR activity within infected population (mRFP(+) and/or Venus(+)) was evaluated by flow cytometry at 3 dpi. (b) CD4+ T cells from a healthy donor were infected with LTR–*Tat*–IRES–*Venus*–EF1α–*mRFP* virus. Flow cytometry plots represent Venus level within live, CD4(+), and mRFP(+) and/or Venus(+) cells, based on the FSC/SSC and fluorescence profiles of the complete culture at 3 dpi. T cell activation was accomplished by treating the anti-CD3/CD28 antibodies for 3 days. Data are representative of three independent experiments.

contains a frame shift mutation, encodes EGFP in the *nef* region, enabling measurement of the LTR activity by the detection of EGFP fluorescence (Fig. 5a). EGFP activity reached a peak at 3 dpi and then decreased during culture under optimum conditions mainly because of viral cytotoxic effects (Fig. 5b). However, re-expression of EGFP was induced by treatment with TNF-α or HDAC inhibitor TSA at 14 dpi, suggesting the existence of latently infected cells in the EGFP(−) populations (Fig. 5c). This result also suggested that an epigenetic mechanism contributes to the LTR silencing, because HDAC inhibition could effectively reactivate LTR. We found that inhibition of EZH2 by DZNep in this population could also induce EGFP expression, indicating that the small population epigenetically remained as a latent population (Fig. 5c). Intriguingly, T cell activation could reactivate the EGFP(+) population at 3 days post single-round virus infection (Fig. 5d–e). The reactivatable population size in PMA/Ionomycin treatment was larger than that of the EGFP expressing population at 4 days under normal cultivation, suggesting that silent integration occurs at the early time point of HIV-1 infection (Fig. 5e).

To address the PRC2 function in latency establishment in HIV-1 infection, we performed EZH2 and SUZ12 knockdown prior to infection of the single-round HIV-1 (Fig. 5f). Similar infectivity of HIV-1 was confirmed by Alu-PCR (Fig. 5g). Transition of EGFP expression revealed that the LTR activity was higher in EZH2- or SUZ12-knockdowned cells than the control cells (Fig. 5h). Furthermore, pre-treatment with DZNep and VPA showed similar results (Fig. 5h–j). Collectively, the results suggested that PRC2 negatively regulates the LTR activity immediately after integration of HIV-1, which may contribute to the establishment of silent integration.

Epigenetic suppression in actively integrated population. After infection of the reporter virus, the LTR activity in the actively infected population was gradually reduced during long-term culture (Figs. 1d and 6a). At 60 dpi, actively Venus expressing population was significantly decreased, resulting in substantial silencing of the LTR. ChIP assay revealed progressive gain of suppressive histone methylations in H3K27 and H3K9 during establishment of global latency (Fig. 6b). In addition, loss of the H3Ac marker indicated an epigenetic shift in transcriptional silencing. In contrast, the status of DNA methylation at the LTR region did not change over a long period (data not shown). Indeed, treating the SAHA or DZNep clearly prevented LTR silencing in the originally LTR active population (Fig. 6c). We further addressed the usefulness of a next generation EZH2 inhibitor, GSK126[34], in HIV-1 reactivation. GSK126 can specifically inhibit EZH2 activity. As a result, the GSK126-treated culture retained the Venus(+) population (Fig. 6c). Taken together, our results of the new reporter virus demonstrated that the transcriptional silencing of HIV-1 is established by two distinct mechanisms. A part of the infected cells possess epigenetically silenced LTR from the beginning of the infection. HIV-1 with a residual population is also epigenetically suppressed during long period. We found a significant difference in sensitivity against exogenous stimulation between the two distinctly infected populations. We compared the time-dependent silenced population from active infection (Venus(+) population) and the originally silenced population (Venus(−) population) by stimulating with TNF-α or PMA/Ionomycin. As a result, the LTR in the gradually silenced population was easily reactivated by exogenous stimulation. In contrast, the originally silenced LTR showed low sensitivity (Fig. 6d). We also treated the distinct population cultures with DZNep, VPA, or SAHA. As results, both populations could be significantly reactivated by the epigenetic drug combination (Fig. 6e). Of note, the time-dependent suppressed LTR was more susceptible than the immediately silenced population. GSK126 treatment in latently LTR also resulted in effective restoration of the LTR activity in both populations (Fig. 6e). These data collectively suggest that the heterogeneous mechanisms of HIV-1 silencing exist; one of them is established immediately after integration. Another mechanism is gradually formed in a time-dependent manner and is more susceptible to signal activation or epigenetic reconstruction. Histone modifications appear to be one common molecular mechanism. We further confirmed LTR reactivation in the latently infected resting CD4+ T cell population by T cell activation signal and epigenetic drugs (Fig. 6f).

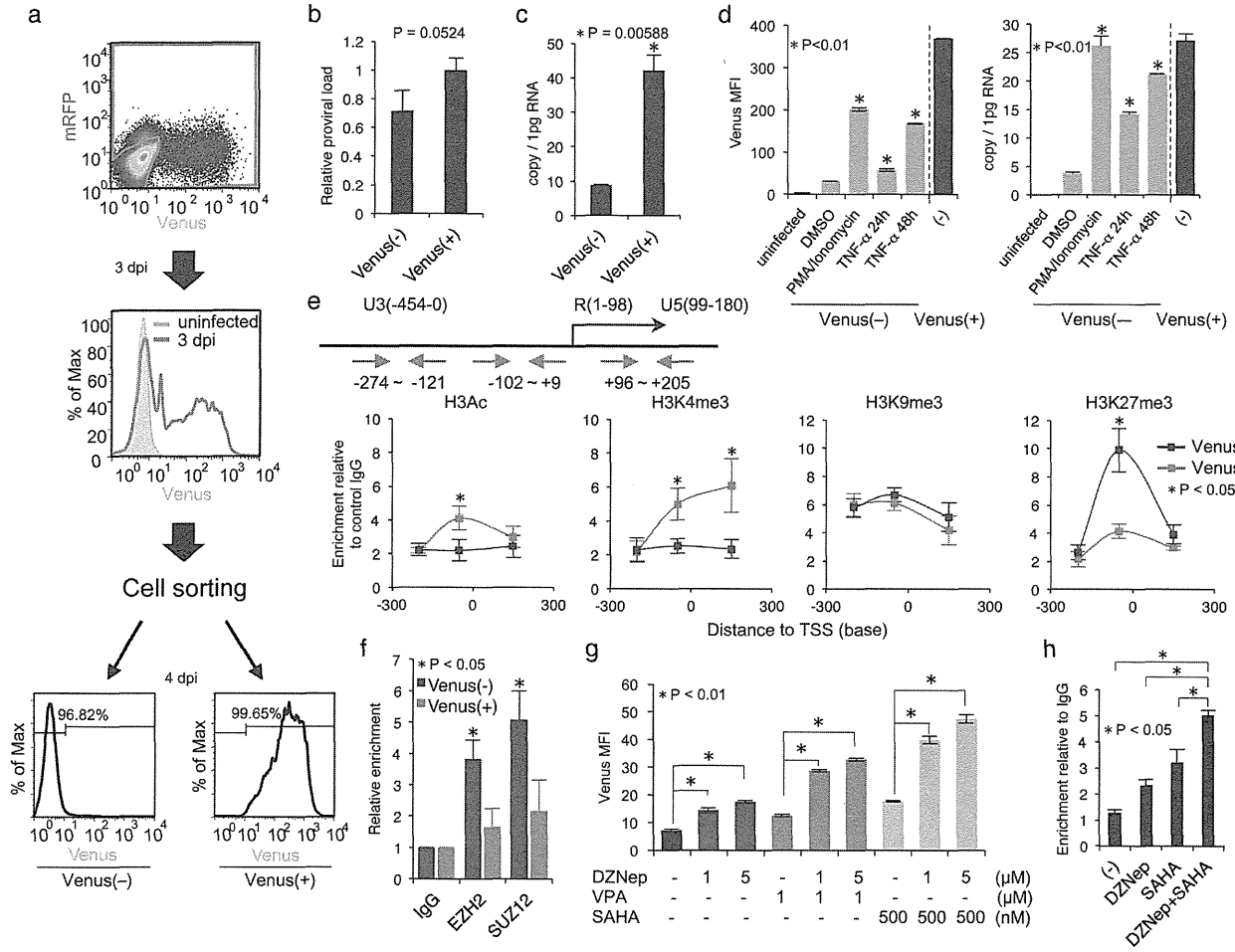

Figure 3 | Epigenetic heterogeneity in HIV-1-infected sub-population. (a) An experimental strategy to investigate molecular basis of LTR silencing. Jurkat cells infected with the LTR–*Tat*–IRES–*Venus*–EF1α–*mRFP* were sorted based on Venus and mRFP fluorescences at 3 dpi. The post-sorted populations were cultured individually and then subjected into molecular analyses (n = 3, representative data). (b) Proviral load from the both infected populations (10 dpi) was evaluated by Alu-PCR method (n = 3, mean ± SD). Albumin DNA was also analyzed as an internal standard. (c) *Venus* mRNA amount was absolutely quantified in Venus(−) and Venus(+) populations (n = 3, mean ± SD). *β-actin* mRNA level was measured as an internal control. (d) The Venus(−) population (20 dpi) was treated with PMA/Ionomycin (24 hours) or TNF-α (24 and 48 hours). Venus MFI (left) and absolute *Venus* mRNA amount (right) were determined (n = 3, mean ± SD). (e) ChIP assay. Histone covalent modifications at LTR region in the sorted Venus(+) and Venus(−) sub-populations were analyzed by PCR-based ChIP assay at 13 dpi. Positions of primer sets for the real-time PCR are indicated in upper diagram. H3 acetylation (AcH3), H3K4 trimethylation (H3K4me3), H3K9 trimethylation (H3K9me3), and H3K27 trimethylation (H3K27me3) were analyzed using specific antibodies. Enrichment values relative to control IgG and LTR positions are plotted (n = 3, mean ± SD). (f) The two distinct populations (13 dpi) were subjected in ChIP assay with anti-EZH2, anti-SUZ12, and control antibodies (n = 3, mean ± SD). (g,h) Venus(−) population (20 dpi) was treated with indicated dose of PRC2 inhibitor DZNep and HDAC inhibitors VPA and SAHA for 48 hours. The reactivated Venus MFI (g) and CTD-phosphorylated Pol II occupancy (h) were evaluated by flow cytometry and ChIP assay, respectively (n = 3, mean ± SD).

Polycomb-mediated epigenetic silencing of HIV-1. The results of the new reporter virus prompted us to address the PRC2 contribution in the establishment of HIV-1 latency. Therefore, we utilized two additional latency models, Hela/LTR-luciferase and U1 cells, to analyze the PRC2 function in the regulation of HIV-1 latency. Knockdown of the PRC2 factors, EZH2 and SUZ12, released the LTR activity in HeLa cells (Fig. 7a–b). In addition, SUZ12 depletion led to increased sensitivity against the Tat protein (Fig. 7c) and *vice versa*. Indeed, enforced SUZ12 expression by plasmid transfection suppressed Tat-dependent LTR transactivation (Fig. 7d). Similar results were obtained from the U1 cell, which was chronically infected with HIV-1[35]. Knockdown of EZH2 or SUZ12 altered histone methylation levels at the promoter region of host *MYT1*, whose expression was constantly regulated by a PRC2-mediated epigenetic mechanism (Fig. 7e–f). In these PRC2-knockdowned cells, the H3K27me3 mark at the LTR region was substantially diminished (Fig. 7g). Viral gene transcription was activated in EZH2- and SUZ12-knockdown cells. These cells showed high sensitivity against TNF-α stimulation, suggesting that PRC2-dependent histone methylation significantly affected viral gene regulation (Fig. 7h). Depletion of PRC2 function did not have any effects on other histone markers. Collectively, PRC2 is a host restriction complex at the establishment and maintenance of LTR silencing by regulating epigenetic states in the LTR region.

Discussion

So far, many researchers have developed original models to investigate the mechanism of HIV-1 latency and revealed several molecular states of the stably silenced 5′LTR sequence[36]. However, a detailed mechanism in the establishment step of the transcriptional dorm-

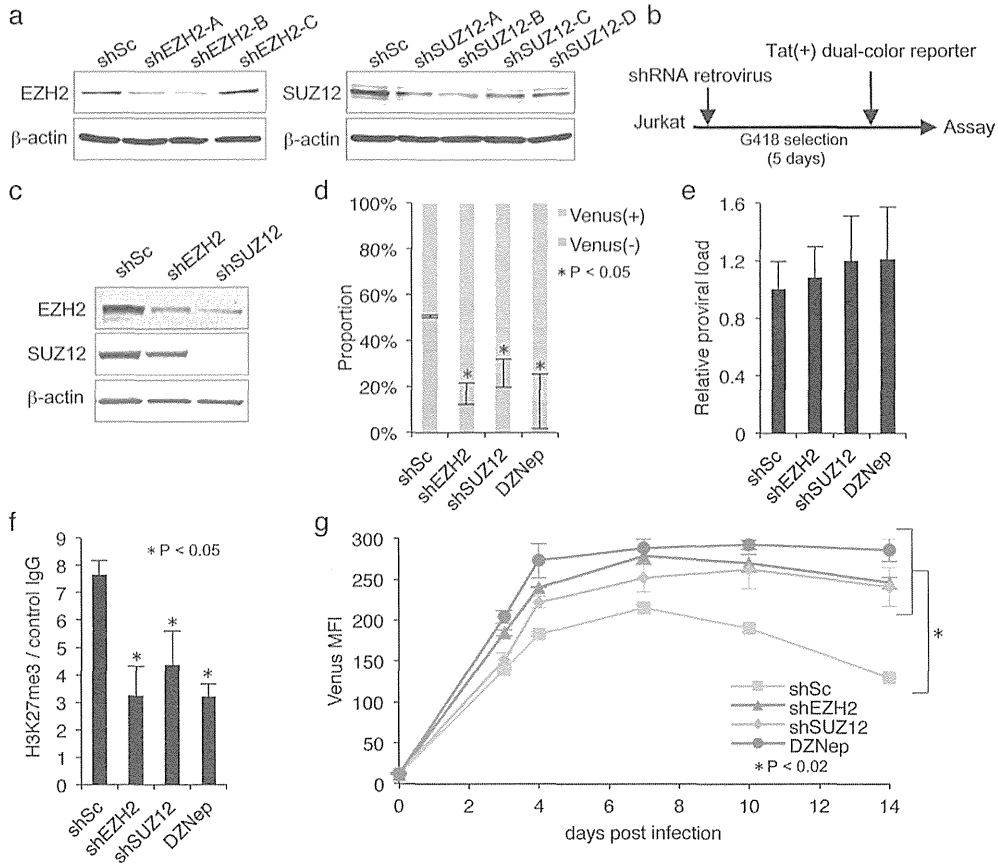

Figure 4 | Involvement of PRC2 in silencing establishment. (a) Previously confirmed shRNAs targeting *EZH2* and *SUZ12* were introduced in Jurkat cells by retrovirus vectors. Western blots showed knockdown efficiencies of the EZH2 (left) and SUZ12 (right). shSc indicates a scrambled control shRNA[32]. β-actin was evaluated as an internal control. Original data are presented in Supplementary Figure 2. shEZH2-A and shSUZ12-A are mainly used for the following experiments. (b) An experimental procedure to examine the role of PRC2 in HIV-1 silencing. Prior to the dual-color reporter infection, knockdown of PRC2 factors was accomplished by retrovirus-mediated shRNA expression. The *Tat*(+) dual-color reporter virus was then inoculated into the EZH2- or SUZ12-depleted Jurkat cells. (c) Knockdown efficiencies of EZH2 and SUZ12 were confirmed by Western blots. Original data are presented in Supplementary Figure 2. (d) Proportional size of Venus(+)/Venus(−) were determined at 4 dpi by flow cytometry (n = 3, mean ± SD). (e) Proviral load from the PRC2-depleted infected populations (4 dpi) evaluated by Alu-PCR (n = 3, mean ± SD). (f) H3K27me3 level on LTR region at 4dpi (n = 3, mean ± SD). (g) The shRNA-expressing and reporter-infected cells were continuously cultured and profiled the Venus/mRFP expression. Venus MFI within infected population was plotted for 14 dpi (n = 3, mean ± SD).

ancy is not fully understood, because of the low frequency of cells harboring silenced HIV-1 and lack of methods to detect such populations in the early phase of HIV-1 infection. In this study, we developed a new reporter virus that carries two different fluorescent genes downstream in LTR and constitutive promoter EF1α, enabling us to analyze the dynamic regulation of the LTR activity. It also allowed us to address a series of epigenetic changes in a fixed, integrated LTR sequence because of the absence of new infection and toxicity from viral gene expression. The Alu-PCR method ensured proviral integration in the interested populations. Using the unbiased model, we identified two ways of transcriptional repression of HIV-1, i.e., expeditious disappearance and continuous decline of HIV-1 gene expression. Surprisingly, one infected population showed very low LTR activity immediately after infection in various cell types, including T cell lines and primary CD4+ T cells (Fig. 2). NL4-3 strain-derived single-round HIV-1 also produced a similar LTR-repressed population at the early phase of T cell infection (Fig. 5). However, the other population presented strong LTR promoter activity immediately after infection, which was gradually suppressed during long-term cultivation (Fig. 6).

Accumulated evidence suggests that host epigenetic factors appear to restrict gene expression from HIV-1 provirus and its propagation in chronically infected individuals[26,37]. However, mechanistic insight into the establishment of transcriptional latency has not been implicated because most previous studies have used stably silenced LTR models. Making use of the traits of the new dual-color reporter mentioned above, we could visualize the epigenetic heterogeneity in LTR at the latency establishment step. Evaluation of covalent histone markers revealed that trimethylation at H3K27 was significantly accumulated at the early phase of infection, particularly the promoter region of LTR in the quickly silenced population. H3K9 trimethylation, which involved transcriptional repression, was not different between the two populations at the early point. H3K27 methylation is catalyzed by PRC2 factors including EZH2, SUZ12, and EED. Recently, Friedman et al. reported the involvement of EZH2 in the maintenance of HIV-1 silencing by using their latent model Jurkat E4 clone[38]. It has been noted that the HIV-1 provirus is preferentially integrated in the euchromatic region where basal transcription activity is dynamically regulated by PRC2-mediated H3K27me3[32,39,40]. We prevented PRC2 function by treating with DZNep or the novel EZH2 inhibitor GSK126 and could elevate LTR activity from the immediate silent population (Fig. 3g and 6e). shRNA-directed EZH2 depletion prior to LTR integration resulted in an imbalance of immediate silent and active infections

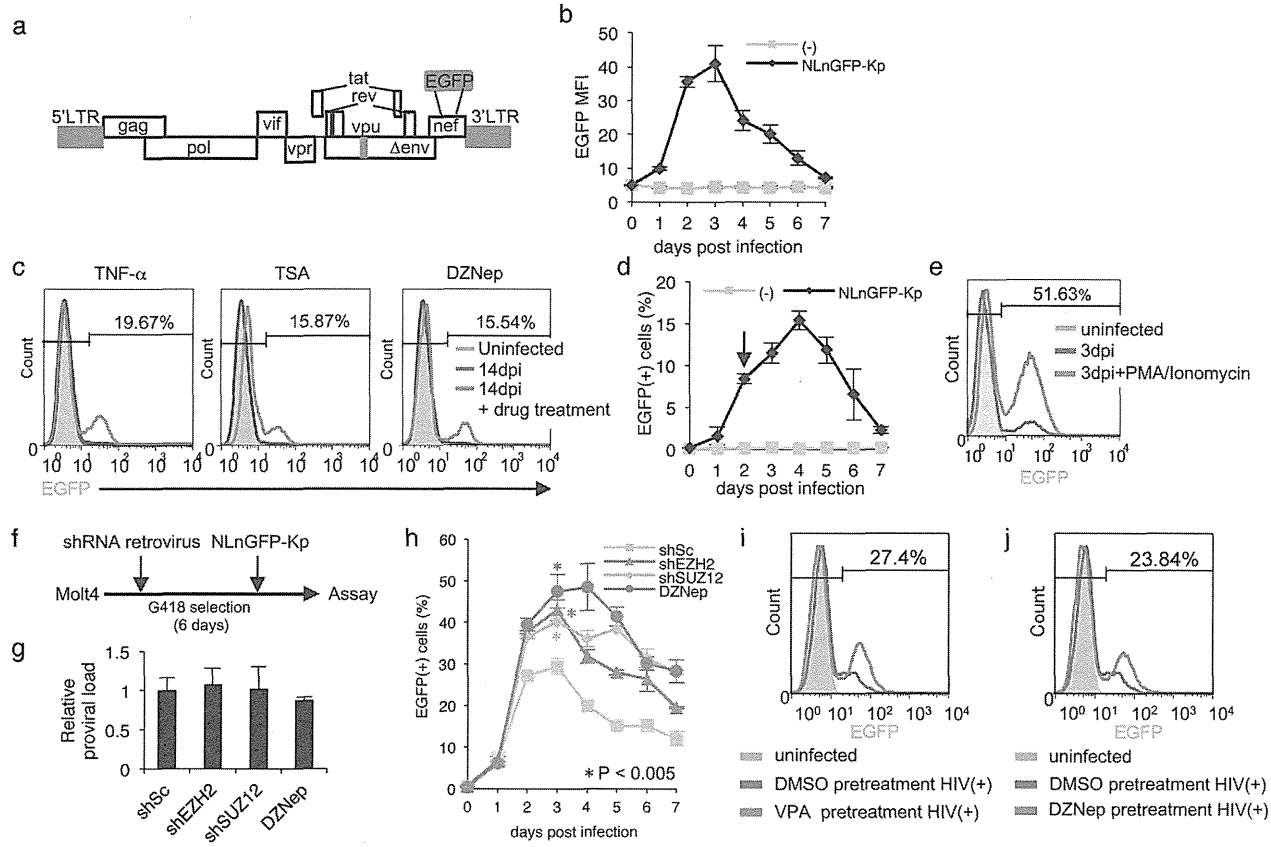

Figure 5 | Latency establishment in single-round HIV-1. (a) Proviral structure of a single-round HIV-1 pNLnGFP-Kp[31]. The concentrated, VSV-G-pseudotyped virus could be effectively introduced in targeted T cell lines. The LTR activity could be directly monitored by EGFP detection. (b) Molt4 T cell line was infected with the single-round HIV-1. After washout of residual viruses, the cells were continuously cultured under the normal condition. The EGFP MFI was determined by flow cytometry (n = 3, mean ± SD). (c) Molt4 cells infected with the single-round HIV-1 were treated with TNF-α (10 ng/ml, 16 hours), TSA (500 nM, 16 hours), or DZNep (5 μM, 48 hours) at 14 dpi. The reactivated population size was defined as EGFP positivity. Data are representative of three independent experiments. (d,e) CCRF-CEM cells were infected with the single-round HIV-1 and analyzed the EGFP(+) population size (n = 3, mean ± SD) (d). Arrow indicates time point of drug treatment. The infected cells (2 dpi) were treated with PMA (100 ng/ml)/Ionomycin (1 μM) for 24 hours. The EGFP expression pattern was determined by flow cytometry at 3 dpi (Data are representative of three independent experiments) (e). (f–h) Influence of PRC2 pre-inhibition. Molt4 cells were infected with the shRNA-expressing retroviruses prior to infection of the single-round HIV-1 (f). The viral DNA was quantified by Alu-PCR at 2 dpi (n = 3, mean ± SD) (g). After the single-round HIV-1 infection, the EGFP expression was continuously examined by flow cytometry (n = 3, mean ± SD) (h). (i,j), Jurkat cells were pre-treated with VPA (i) and DZNep (j) for 48 hours and then infected with the single-round HIV-1. EGFP expression levels were evaluated at 3 dpi (Data are representative of three independent experiments).

(Fig. 4). The fact that the decline of SUZ12 led to the same result indicated the importance of the complex-dependent epigenetic manner in the immediate silencing. ChIP assay with EZH2 and SUZ12 antibodies demonstrated occupancy of the PRC2 factor at transcription start site (TSS) in LTR (Fig. 3f). Collectively, our data suggest that PRC2-dependent epigenetic control of LTR is involved in the establishment of immediate silent infection. In contrast, silencing-associated DNA methylation was not detected in our model. Importantly, we also observed that major active histone modifications, H3K4 trimethylation and histone acetylation, were significantly higher in the actively infected population than the immediately silenced population (Fig. 3e). Indeed, HDAC inhibitors such as VPA and SAHA, which are implicated as new drugs to purge latently infected cells[41], could reactivate LTR. Of note, cooperation of histone acetylation and H3K27me3 appeared to coordinate the actual LTR activity (Fig. 3g, 6e–f). Further study about H3K4me3 and its regulator trithorax group, which is a cellular counterpart of polycomb, may help to understand the molecular basis of the early step of HIV-1 regulation.

Time-dependent regression of the LTR activity has certainly been implicated. Because this reporter does not express toxic viral genes and expresses fluorescent proteins enabling us to purify the populations involved, we addressed the dynamic course of LTR repression in the actively infected population. Expectedly, the LTR activity within the active population gradually reduced during culture under normal conditions. Interestingly, ChIP assay revealed that H3K27me3 accumulated at the LTR region in the time-dependent silenced population was similar to the immediately silent population (Fig. 6b). These data suggest that PRC2-mediated H3K27me3 and its negative gene regulation may contribute to HIV-1 silencing between the early phase establishment and late phase maintenance of HIV-1 latency. Whereas, the acquisition of H3K9me3, which has already been implicated in HIV-1 latency[42,43], appears to be involved in late stage maintenance of HIV-1 latency. Importantly, LTR responses to epigenetic drugs and exogenous stimuli clearly differed in the two distinct populations. We found that the repressed LTR in the originally active infection population was highly sensitive not only to NF-κB stimulators but also to epigenetic drugs compared with the

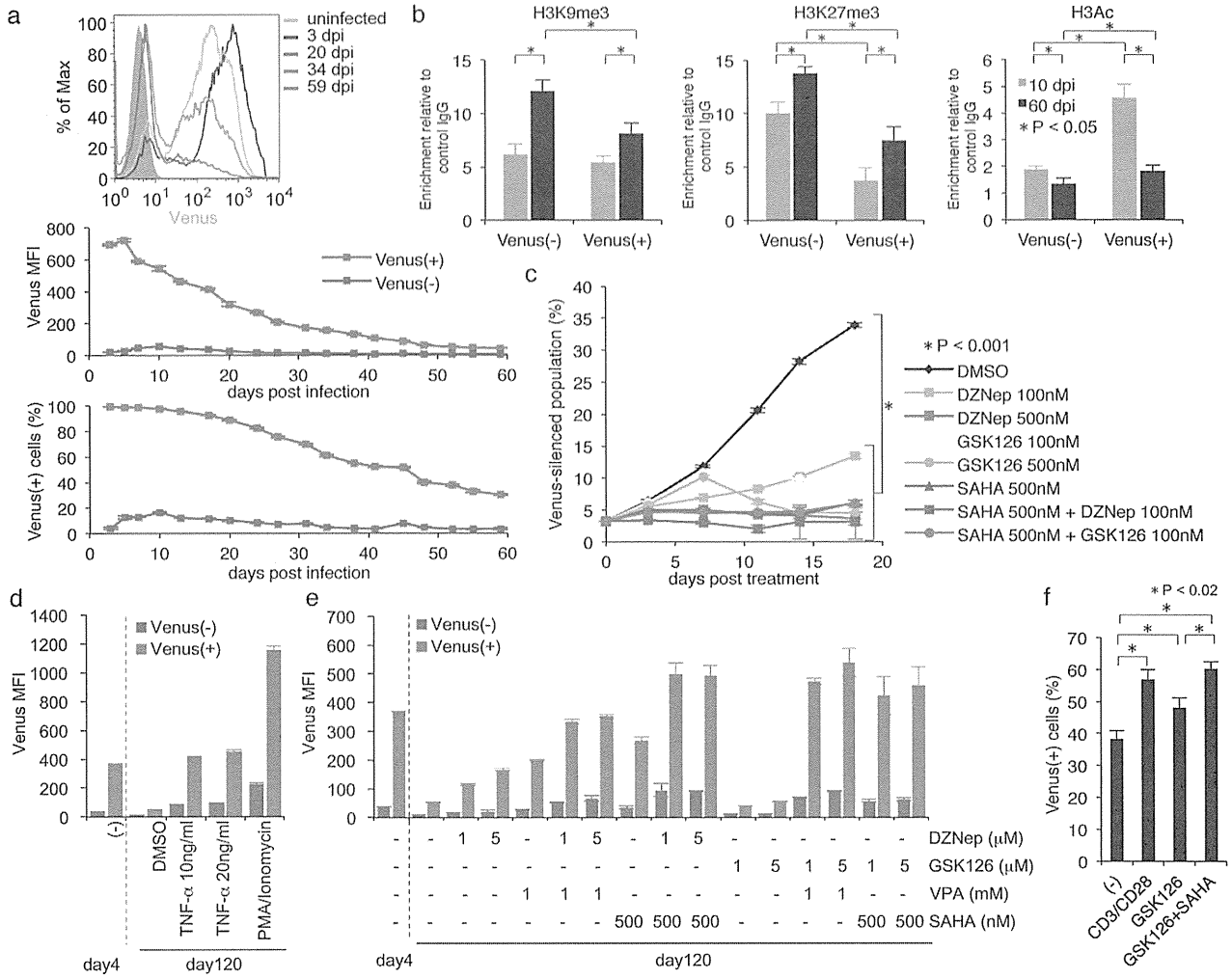

Figure 6 | LTR silencing in actively infected cells. (a) Jurkat cells were infected with the LTR–*Tat*–IRES–*Venus*–EF1α–*mRFP* virus. The Venus(+) population was sorted based on the Venus expression at 3 dpi and cultured individually for 60 days. LTR activity was evaluated by Venus expression level. The flow cytometry histograms (upper histogram) and the progress of MFI (middle graph) and proportion of Venus(+) population (lower graph) are presented (red line). The progress of immediately silenced population is also depicted (blue line) (n = 3, mean ± SD). (b) ChIP assay with indicated antibodies at 10 and 60 dpi revealed changes of the histone modifications at the LTR promoter region in the immediately silenced population (shown as Venus(−)) and the time-dependent silenced population (shown as Venus(+) (n = 3, mean ± SD). (c) The sorted Venus(+) population at 7 dpi was treated with the epigenetic drug combination for 18 days. The transition of Venus expression was examined by flow cytometry. The population size of Venus-silenced cells was plotted (n = 3, mean ± SD). (d,e) The time-dependent silenced population from active infection (Venus(+), red bar) and the originally silenced population (Venus(−), blue bar) were treated with TNF-α or PMA/Ionomycin for 24 hours (d) and DZNep, VPA, or SAHA for 48 hours or GSK126 for 96 hours (e) at 120 dpi. The LTR activity was evaluated by Venus MFI (n = 3, mean ± SD). (f) Resting CD4+ T cells were infected with the dual-color reporter virus and then reactivated with indicated drugs for 3 days. Venus(+) population size within the infected cells at 6 dpi were shown (n = 3, mean ± SD).

immediately silent population (Fig. 6d–e). In addition to the epigenetic regulation, other mechanisms such as integration site preferences or differences in host factor expression could be associated with determining the robustness of LTR latency[44–48]. Of late, noninduced HIV-1 provirus was identified in clinical samples[49]. The strong suppression appeared to occur by transcriptional dormancy, leading to an underestimation of latent reservoir size based on a T cell activation survey. The immediately silenced population that we identified in this study might explain this concept. By combining our reporter system with massively parallel DNA sequencing or comprehensive expression profiling, we will be able to clarify the residual question in the near future.

In the context of an epigenetic maintenance in LTR regulation, components of the polycomb family appear to be categorized as host restriction factors because SUZ12 overexpression inhibited Tat-mediated LTR activation, and *vice versa* in stable latent models (Fig. 7). PRC2 has central roles in the regulation of expression of a number of host genes[50]. We recently reported that aberrant activation of PRC2 leads to microRNA suppression, which in turn activates NF-κB signaling in T cells[51]. Understanding the accurate regulatory mechanism and function of PRC2 in T cells may be helpful for intervention of latent HIV-1. It is also necessary to understand the molecular mechanisms of how PRC2 is recruited to LTR in the latency population. Recruiters of mammalian PRC2 appear to be locus specific and still largely unknown. In addition, one major challenge is to delineate the role of Tat in epigenetic regulation of LTR. Absence of *Tat* creates robust latent population (Fig. 1). Because Tat fluctuation drives phenotypic diversity[52], interplay between host epi-

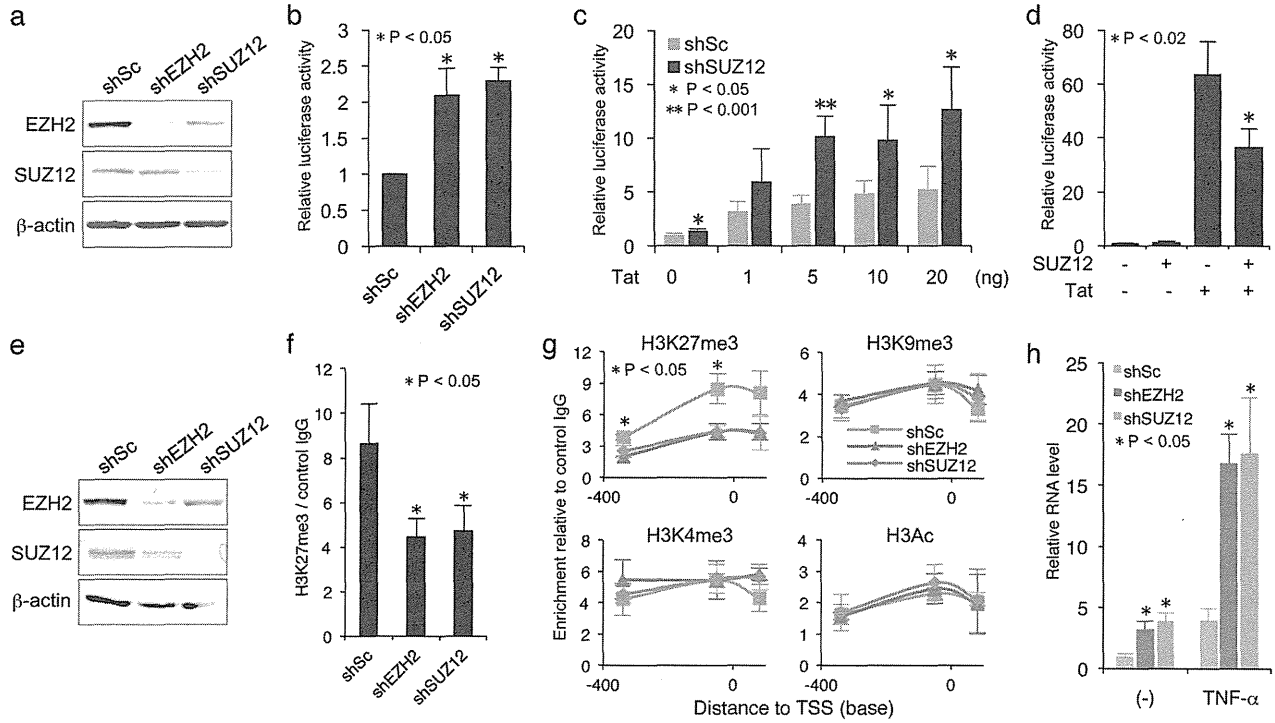

Figure 7 | Role of PRC2 in LTR regulation. (a–d) PRC2 contributes to LTR silencing in HeLa/LTR-luciferase cells. HeLa/LTR-luciferase cells were infected with the shSUZ12-, shEZH2-, or scrambled shRNA (shSc)-expressing retrovirus. Knockdown efficiency was confirmed by Western blots (a, original data are presented in Supplementary Figure 2). The LTR activities of the knockdowned cells were examined by luciferase assay (n = 3, mean ± SD) (b). HeLa/LTR-luciferase cells with shSUZ12 or shSc were transfected with various dose of Tat expression plasmid DNA. The luciferase activity was evaluated at 24 hours post transfection (n = 6, mean ± SD) (c). HeLa/LTR-luciferase cells were transfected with the plasmid DNA encoding Tat or SUZ12. The luciferase activity was examined at 24 hours post Tat transfection (n = 6, mean ± SD) (d). (e–h) PRC2 contributes to HIV-1 silencing in U1 cells. The U1 cells were infected with the retrovirus expressing shEZH2, shSUZ12, or shSc. (e) Western blots confirmed depletion of EZH2 or SUZ12. Original data are presented in Supplementary Figure 2. (g,f) ChIP assay showed PRC2 knockdown-associated alterations of the H3K27me3 level at *MYT1* promoter region and the various histone modifications at LTR region (n = 3, mean ± SD). (h) Relative *gag* RNA levels in shRNA-expressing U1 cells in the presence or absence of TNF-α (10 ng/ml, 48 hours) (n = 3, mean ± SD).

genetic factors and viral factors may dominate the integrated LTR activity.

Resting CD4+ T cells are largely non-permissive for HIV-1 replication because of high activity of triphosphohydrolase SAMHD1[53] and rigid actin cortex barrier[54]. To simply examine the dynamic activity and epigenetic state of LTR integrated in the quiescent primary CD4+ T cells, we performed reporter infection in non-activated CD4+ T cell by using the rigorously concentrated dual-color reporter virus, which is derived from single-round high-titer lentivirus system[55]. Spinoculation method[56] facilitates viral entry and following integration in resting CD4+ T cell. Figure 2b have shown the heterogeneity of LTR activity in resting CD4+ T cells. It clearly reflected that number of cells having Venus expression increased upon CD3/CD28 stimulation, indicating that many cells are productive as compared to the resting stage. There are many articles, which support this observation *in vitro* and *in vivo*.

Taken together, results from studies with new reporter and some latent models have illustrated that PRC2 plays key roles in the establishment and maintenance of virus transcriptional repression. The distinct ways of infection produced at least two latently infected populations. Although the clinical importance of these populations is still open to question, our findings raise the interesting possibility that PRC2 depletion reduces the size of the deeply inactivated virus population (Fig. 4). Furthermore, co-treatment with PRC2 and HDAC inhibitors more effectively restored the silenced LTR activity in both cell line models and resting CD4+ T cells. Our observations suggest that PRC2 inhibition may be a valuable future strategy to prevent establishment of HIV-1 silencing and eliminate latent reservoirs, which is an urgent challenge in HIV studies. Because epigenetic markers are potentially reversible, genuine epigenetic-targeted therapy may hold great promise for HIV-1 eradication.

Methods

Cell culture and drug treatments. Jurkat, Molt4, CCRF-CEM, SupT1 and U1 cells were maintained in RPMI1640 medium (GIBCO) with 10% fetal bovine serum (FBS, GIBCO), and antibiotics (GIBCO). For exogenous stimulation, the cells were treated with PMA (LC Laboratories), Ionomycin (CALBIOCHEM), or TNF-α (R&D systems). For inhibition of epigenetic factors, the cells were treated with the indicated concentrations of VPA (SIGMA), SAHA (Cayman), TSA (SIGMA), 3-deazaneplanocin A (DZNep, Cayman), or GSK126 (Chemie Tek). HEK293T, HEK293FT, and Hela/LTR-luciferase cells were maintained in DMEM with 10% FBS and antibiotics. Human peripheral blood mononuclear cells (PBMCs) were prepared from whole blood of healthy donors by density gradient centrifugation with Ficoll-Paque (GE healthcare). CD4+ T cells were purified by CD4+ T cell isolation kit (Miltenyi Biotec) and maintained in RPMI1640 with 10% of FBS. T cell activation was accomplished by treating the anti-CD3/CD28 antibodies (Miltenyi Biotec).

Generation and transduction of dual-color reporter virus. For generation of the dual-color reporter lentivirus DNA, Replication-defective, self-inactivating lentivirus vectors CSII–EF–MCS–IRES2–Venus and CS–RfA–EF–mRFP1 were used[55]. DNA primers used for generating the vectors are described in supplementary information. HIV-1 LTR sequence was obtained from genomic DNA of HIV-1 NL4-3-infected Molt4 cells by PCR amplification with a primer set (AgeI LTR forward and AgeI LTR reverse). The amplified LTR DNA was inserted into an EF1α promoter region of the CSII–EF–MCS–IRES2–Venus plasmid. Tat cDNA from HIV-1 NL4-3 was amplified by PCR with a primer set (NotI Tat forward and BamHI Tat reverse) and inserted into NotI and BamHI sites within CSII–LTR–MCS–IRES2–Venus plasmid. The established LTR–Tat/empty–IRES2–Venus sequence was amplified by PCR with primers (SalI LTR-Tat-IRES-Venus For and XbaI LTR-Tat-IRES-Venus Rev),

followed by cloning into pENTR4-H1 vector at SalI and XbaI sites. The produced entry vector was recombined with a CS–RfA–EF–mRFP1 vector by Gateway LR Clonase II Enzyme Mix (Invitrogen).

For production of reporter virus, the accomplished lentiviral plasmid vector (CS–LTR–*Tat*/empty–IRES–*Venus*–EF–*mRFP*) was co-transfected with the packaging plasmids (pCAG-HIVgp and pCMV-VSV-G-RSV-Rev) into 293FT cells. High-titer viral solutions were prepared by centrifugation-based concentration at 8,000 × *g* for at least 3 hours and used for transduction into target cells. 1×10^6 cells were infected with the lentivirus by spinoculation method (1,800 rpm, 2 hours) and then cultured in 2 ml of RPMI1640 with 10% FCS. For primary CD4+ T cells, approximately 20 ml of VSV-G-pseudotyped reporter virus solution from the transfection supernatant were concentrated by centrifugation and used for 1×10^6 primary T cells.

Single-round HIV infection. A single-round HIV molecular clone pNLnGFP-Kp[57] was provided from Prof. A. Adachi, Tokushima University, Japan. The plasmid and the VSV-G- and Rev-expressing vector were co-transfected into 293FT cells. At 48 hours post-transfection, the culture supernatant was 0.45 μm filtrated and concentrated by centrifugation at 8,000 × *g*, 3 hours at 4°C. The collected virus solution was immediately used or kept in −80°C freezer.

Flow cytometric analysis. Expression levels of florescent proteins were analyzed by FACSCalibur (BD). The reporter-introduced cells were harvested and re-suspended in 0.3% FBS/PBS. LTR activity in the infected population was defined by calculating the expression levels of Venus (FL1) and mRFP (FL3). For EGFP detection, the single-round HIV-infected cells were fixed by 3% formaldehyde before flow cytometry. CD4+ T cells were defined by staining with APC-conjugated anti-Human CD4 antibody (BD, 551980)

Chromatin immunoprecipitation (ChIP) assay. Histone covalent modifications were quantified by PCR-ChIP assay[58] with some modifications. Briefly, the cells (1×10^6) were cross-linked with 1% formaldehyde for 15 min at room temperature, washed with PBS at 4°C, and suspended in SDS-lysis buffer (50 mM Tris-HCl, 1% SDS, 10 mM EDTA, pH 8.1, protease inhibitor cocktail). The lysate was then sonicated on ice for 1 min 40 sec (Astreson ultrasonic processor, MISONIX Inc.). After centrifugation, the supernatants were subjected to immunoprecipitation with specific antibodies; anti-H3K27me3 (Active Motif, #39155), anti-H3K9me3 (Abcam, #ab8898-100), anti-H3K4me3 (Cell Signaling, #9751S), anti-AcH3 (Millipore, #06-599), anti-EZH2 (Cell Signaling, #5246S), anti- SUZ12 (Cell Signaling, #3737S), anti-CTD-phosphorylated Pol II (COVANCE, MMS-134R), anti-normal Rabbit IgG (Cell Signaling, #2729S). The precipitated DNA was purified and analyzed by real-time PCR with specific primers (supplementary information).

Retroviral shRNA knockdown. shRNA-expressing retroviral vector (pSINsi-U6, TAKARA, Japan) was used for EZH2 and SUZ12 knockdowns. The specific retroviral vectors were established by insertion of synthesized oligonucleotides using BamHI and ClaI sites. Sequences of the inserted oligonucleotides have previously been tested (supplementary information). Retrovirus production was carried out in 293T cells with the pSIN vector, pGP vector (*gag-pol* coding, TAKARA), and pCMV-VSV-G-RSV-Rev. At 48 hours post-transfection, the retrovirus solution was 0.45 μm filtrated, concentrated by centrifugation, and added to target cells for 24 hours establishment. The transduced cells were selected with 0.5 mg/ml of G418 for 5–6 days.

Western blotting. Whole cell lysates were analyzed by 7.5 to 10% acrylamide Tris-HCl buffered SDS-PAGE. Western blots were performed with first antibodies listed below; β-actin (SantaCruz Biotechnology, sc-8432), EZH2 (Cell Signaling, #3147S), SUZ12 (Cell Signaling, #3737S). Alkaline phosphatase-conjugated anti-mouse or anti-rabbit IgG was used as a secondary antibody. BCIP/NBT substrate (Promega) with ALP buffer (100 mM Tris-HCl pH 9.5, 100 mM NaCl, 50 mM $MgCl_2$) was used for detection.

PCR. Total RNA isolation was performed using ISOGEN (Wako, Japan). The DNaseI-treated total RNA was subjected to reverse-transcriptase (RT) reaction using SuperScript II (Invitrogen) with manufacturer's protocol. The oligo dT primers-based synthesized cDNA was analyzed by quantitative PCR using real-time PCR system (Thermal cycler Dice, TAKARA). The specific PCR was performed using gene-specific primers and SYBRGreen (TAKARA). The level of *β-actin* was quantified for internal control. Absolute copy number was determined by standard curve method. Genomic DNA in each infected population was extracted using QIAamp DNA Blood Mini Kit (QIAGEN). Alu-based PCR was performed to quantify integrated HIV-1 provirus, as previously described[59].

Reporter gene assay. HeLa/LTR-luciferase cells were previously established[58]. The firefly luciferase activity was analyzed by luciferase reporter assay system (Promega) and normalized by protein concentration of cell lysate.

1. Perelson, A. S. *et al.* Decay characteristics of HIV-1-infected compartments during combination therapy. *Nature* **387**, 188–191 (1997).
2. Gulick, R. M. *et al.* Treatment with indinavir, zidovudine, and lamivudine in adults with human immunodeficiency virus infection and prior antiretroviral therapy. *N. Engl. J. Med.* **337**, 734–739 (1997).
3. Finzi, D. *et al.* Identification of a reservoir for HIV-1 in patients on highly active antiretroviral therapy. *Science* **278**, 1295–1300 (1997).
4. Wong, J. K. *et al.* Recovery of replication-competent HIV despite prolonged suppression of plasma viremia. *Science* **278**, 1291–1295 (1997).
5. Chun, T. W., Davey, R. T., Jr, Engel, D., Lane, H. C. & Fauci, A. S. Re-emergence of HIV after stopping therapy. *Nature* **401**, 874–875 (1999).
6. Chun, T. W. *et al.* Presence of an inducible HIV-1 latent reservoir during highly active antiretroviral therapy. *Proc. Natl. Acad. Sci. U.S.A.* **94**, 13193–13197 (1997).
7. Bailey, J. R. *et al.* Residual human immunodeficiency virus type 1 viremia in some patients on antiretroviral therapy is dominated by a small number of invariant clones rarely found in circulating CD4+ T cells. *J. Virol.* **80**, 6441–6457 (2006).
8. Kieffer, T. L. *et al.* (2004) Genotypic analysis of HIV-1 drug resistance at the limit of detection: virus production without evolution in treated adults with undetectable HIV loads. *J. Infect. Dis.* **189**, 1452–1465 (2004).
9. Frenkel, L. M. *et al.* Multiple viral genetic analyses detect low-level human immunodeficiency virus type 1 replication during effective highly active antiretroviral therapy. *J. Virol.* **77**, 5721–5730 (2003).
10. Kinoshita, S., Chen, B. K., Kaneshima, H. & Nolan, G. P. Host control of HIV-1 parasitism in T cells by the nuclear factor of activated T cells. *Cell* **95**, 595–604 (1998).
11. Perkins, N. D. *et al.* A cooperative interaction between NF-kappa B and Sp1 is required for HIV-1 enhancer activation. *EMBO J.* **12**, 3551–3558 (1993).
12. Kim, Y. K., Mbonye, U., Hokello, J. & Karn, J. T-cell receptor signaling enhances transcriptional elongation from latent HIV proviruses by activating P-TEFb through an ERK-dependent pathway. *J. Mol. Biol.* **410**, 896–916 (2011).
13. Kao, S. Y., Calman, A. F., Luciw, P. A. & Peterlin, B. M. Anti-termination of transcription within the long terminal repeat of HIV-1 by tat gene product. *Nature* **330**, 489–493 (1987).
14. Wei, P., Garber, M. E., Fang, S. M., Fischer, W. H. & Jones, K. A. A novel CDK9-associated C-type cyclin interacts directly with HIV-1 Tat and mediates its high-affinity, loop-specific binding to TAR RNA. *Cell* **92**, 451–462 (1998).
15. Van Lint, C., Emiliani, S., Ott, M. & Verdin, E. Transcriptional activation and chromatin remodeling of the HIV-1 promoter in response to histone acetylation. *EMBO J.* **15**, 1112–1120 (1996).
16. Williams, S. A. *et al.* NF-kappaB p50 promotes HIV latency through HDAC recruitment and repression of transcriptional initiation. *EMBO J.* **25**, 139–149 (2006).
17. Tyagi, M. & Karn, J. CBF-1 promotes transcriptional silencing during the establishment of HIV-1 latency. *EMBO J.* **26**, 4985–4995 (2007).
18. Jiang, G., Espeseth, A., Hazuda, D. J. & Margolis, D. M. c-Myc and Sp1 contribute to proviral latency by recruiting histone deacetylase 1 to the human immunodeficiency virus type 1 promoter. *J. Virol.* **81**, 10914–10923 (2007).
19. Cohen, J. Exploring how to get at--and eradicate--hidden HIV. *Science* **279**, 1854–1855 (1998).
20. Chun, T. W., Engel, D., Mizell, S. B., Ehler, L. A. & Fauci, A. S. Induction of HIV-1 replication in latently infected CD4+ T cells using a combination of cytokines. *J. Exp. Med.* **188**, 83–91 (1998).
21. Chun, T. W. *et al.* Effect of interleukin-2 on the pool of latently infected, resting CD4+ T cells in HIV-1-infected patients receiving highly active anti-retroviral therapy. *Nat. Med.* **5**, 651–655 (1999).
22. Davey, R. T., Jr. *et al.* HIV-1 and T cell dynamics after interruption of highly active antiretroviral therapy (HAART) in patients with a history of sustained viral suppression. *Proc. Natl. Acad. Sci. U.S.A.* **96**, 15109–15114 (1999).
23. Stellbrink, H. J. *et al.* Effects of interleukin-2 plus highly active antiretroviral therapy on HIV-1 replication and proviral DNA (COSMIC trial). *AIDS* **16**, 1479–1487 (2002).
24. Lafeuillade, A. *et al.* Pilot study of a combination of highly active antiretroviral therapy and cytokines to induce HIV-1 remission. *J. Acquir. Immune Defic. Syndr.* **26**, 44–55 (2001).
25. Lehrman, G. *et al.* Depletion of latent HIV-1 infection in vivo: a proof-of-concept study. *Lancet* **366**, 549–555 (2005).
26. Archin, N. M. *et al.* Administration of vorinostat disrupts HIV-1 latency in patients on antiretroviral therapy. *Nature* **487**, 482–485 (2012).
27. Ruelas, D. S. & Greene, W. C. An integrated overview of HIV-1 latency. *Cell* **155**, 519–529 (2013).
28. Chun, T. W. *et al.* Quantification of latent tissue reservoirs and total body viral load in HIV-1 infection. *Nature* **387**, 183–188 (1997).
29. Ylisastigui, L., Archin, N. M., Lehrman, G., Bosch, R. J. & Margolis, D. M. Coaxing HIV-1 from resting CD4 T cells: histone deacetylase inhibition allows latent viral expression. *AIDS* **18**, 1101–1108 (2004).
30. Ishida, T., Hamano, A., Koiwa, T. & Watanabe, T. 5′ long terminal repeat (LTR)-selective methylation of latently infected HIV-1 provirus that is demethylated by reactivation signals. *Retrovirology* **3**, 69 (2006).
31. Blazkova, J. *et al.* CpG methylation controls reactivation of HIV from latency. *PLoS Pathog.* **5**, e1000554 (2009).
32. Schroder, A. R. *et al.* HIV-1 integration in the human genome favors active genes and local hotspots. *Cell* **110**, 521–529 (2002).
33. Han, Y. *et al.* Resting CD4+ T cells from human immunodeficiency virus type 1 (HIV-1)-infected individuals carry integrated HIV-1 genomes within actively transcribed host genes. *J. Virol.* **78**, 6122–6133 (2004).
34. McCabe, M. T. *et al.* EZH2 inhibition as a therapeutic strategy for lymphoma with EZH2-activating mutations. *Nature* **492**, 108–112 (2012).

35. Emiliani, S. *et al.* Mutations in the tat gene are responsible for human immunodeficiency virus type 1 postintegration latency in the U1 cell line. *J. Virol.* **72**, 1666–1670 (1998).
36. Colin, L. & Van Lint, C. Molecular control of HIV-1 postintegration latency: implications for the development of new therapeutic strategies. *Retrovirology* **6**, 111 (2009).
37. Archin, N. M. *et al.* Expression of latent HIV induced by the potent HDAC inhibitor suberoylanilide hydroxamic acid. *AIDS Res. Hum. Retroviruses.* **25**, 207–212 (2009).
38. Friedman, J. *et al.* Epigenetic silencing of HIV-1 by the histone H3 lysine 27 methyltransferase enhancer of Zeste 2. *J. Virol.* **85**, 9078–9089 (2011).
39. Kouzarides, T. Chromatin modifications and their function. *Cell* **128**, 693–705 (2007).
40. Barski, A. *et al.* High-resolution profiling of histone methylations in the human genome. *Cell* **129**, 823–837 (2007).
41. Geeraert, L., Kraus, G. & Pomerantz, R. J. Hide-and-seek: the challenge of viral persistence in HIV-1 infection. *Annu. Rev. Med.* **59**, 487–501 (2008).
42. du Chene, I. *et al.* Suv39H1 and HP1gamma are responsible for chromatin-mediated HIV-1 transcriptional silencing and post-integration latency. *EMBO J.* **26**, 424–435 (2007).
43. Marban, C. *et al.* Recruitment of chromatin-modifying enzymes by CTIP2 promotes HIV-1 transcriptional silencing. *EMBO J.* **26**, 412–423 (2007).
44. Duverger, A. *et al.* Determinants of the establishment of human immunodeficiency virus type 1 latency. *J. Virol.* **83**, 3078–3093 (2009).
45. Burnett, J. C., Miller-Jensen, K., Shah, P. S., Arkin, A. P. & Schaffer, D. V. Control of stochastic gene expression by host factors at the HIV promoter. *PLoS Pathog.* **5**, e1000260 (2009).
46. Duverger, A. *et al.* An AP-1 binding site in the enhancer/core element of the HIV-1 promoter controls the ability of HIV-1 to establish latent infection. *J. Virol.* **87**, 2264–2277 (2013).
47. Tyagi, M., Pearson, R. J. & Karn, J. Establishment of HIV latency in primary CD4+ cells is due to epigenetic transcriptional silencing and P-TEFb restriction. *J. Virol.* **84**, 6425–6437 (2010).
48. Budhiraja, S., Famiglietti, M., Bosque, A., Planelles, V. & Rice, A. P. Cyclin T1 and CDK9 T-loop phosphorylation are downregulated during establishment of HIV-1 latency in primary resting memory CD4+ T cells. *J. Virol.* **87**, 1211–1220 (2013).
49. Ho, Y. C. *et al.* Replication-competent noninduced proviruses in the latent reservoir increase barrier to HIV-1 cure. *Cell* **155**, 540–551 (2013).
50. Kirmizis, A. *et al.* Silencing of human polycomb target genes is associated with methylation of histone H3 Lys 27. *Genes Dev.* **18**, 1592–1605 (2004).
51. Yamagishi, M. *et al.* Polycomb-mediated loss of miR-31 activates NIK-dependent NF-kappaB pathway in adult T cell leukemia and other cancers. *Cancer Cell* **21**, 121–135 (2012).
52. Weinberger, L. S., Burnett, J. C., Toettcher, J. E., Arkin, A. P. & Schaffer, D. V. Stochastic gene expression in a lentiviral positive-feedback loop: HIV-1 Tat fluctuations drive phenotypic diversity. *Cell* **122**, 169–182 (2005).
53. Baldauf, H. M. *et al.* SAMHD1 restricts HIV-1 infection in resting CD4(+) T cells. *Nat. Med.* **18**, 1682–1687 (2012).
54. Pan, X., Baldauf, H. M., Keppler, O. T. & Fackler, O. T. Restrictions to HIV-1 replication in resting CD4+ T lymphocytes. *Cell Res.* **23**, 876–885 (2013).
55. Miyoshi, H., Takahashi, M., Gage, F. H. & Verma, I. M. Stable and efficient gene transfer into the retina using an HIV-based lentiviral vector. *Proc. Natl. Acad. Sci. U.S.A.* **94**, 10319–10323 (1997).
56. O'Doherty, U., Swiggard, W. J. & Malim, M. H. Human immunodeficiency virus type 1 spinoculation enhances infection through virus binding. *J. Virol.* **74**, 10074–10080 (2000).
57. Fukumori, T. *et al.* Regulation of cell cycle and apoptosis by human immunodeficiency virus type 1 Vpr. *Microbes Infect.* **2**, 1011–1017 (2000).
58. Yamagishi, M. *et al.* Retroviral delivery of promoter-targeted shRNA induces long-term silencing of HIV-1 transcription. *Microbes Infect.* **11**, 500–508 (2009).
59. Brussel, A. & Sonigo, P. Analysis of early human immunodeficiency virus type 1 DNA synthesis by use of a new sensitive assay for quantifying integrated provirus. *J. Virol.* **77**, 10119–10124 (2003).

Acknowledgments

We thank Drs. H. Miyoshi and A. Miyawaki for providing the Venus- and mRFP-encoding lentivirus vectors. This work is supported by JSPS KAKENHI Grant Number 24790436 (M.Y.), 23390250 (T.W.), Grant-in-Aid from the Ministry of Health, Labour and Welfare H24-AIDS-008 (T.W.), and grant from the Uehara Memorial Foundation (M.Y.).

Author contributions

Y.M. and M.Y. performed the all experiments. M.K.I., D.F. and T.I. advised the experimental design and protocols used in this study. T.W. and M.Y. conceived the study, designed the experiments and helped in drafting and finalizing the manuscripts. All authors reviewed the manuscript.

Additional information

Supplementary information accompanies this paper at http://www.nature.com/scientificreports

Competing financial interests: The authors declare no competing financial interests.

How to cite this article: Matsuda, Y. *et al.* Epigenetic Heterogeneity in HIV-1 Latency Establishment. *Sci. Rep.* 5, 7701; DOI:10.1038/srep07701 (2015).

Journal of Infectious Diseases Advance Access published August 6, 2014

MAJOR ARTICLE

Epigenetic Repression of Interleukin 2 Expression in Senescent CD4$^+$ T Cells During Chronic HIV Type 1 Infection

Kaori Nakayama-Hosoya,[1,2] Takaomi Ishida,[3] Ben Youngblood,[5] Hitomi Nakamura,[1,2] Noriaki Hosoya,[1,2] Michiko Koga,[1] Tomohiko Koibuchi,[4] Aikichi Iwamoto,[1,2,3,4] and Ai Kawana-Tachikawa[1]

[1]Division of Infectious Diseases, Advanced Clinical Research Center, [2]International Research Center for Infectious Diseases, [3]Research Center for Asian Infectious Diseases, and [4]Department of Infectious Diseases and Applied Immunology, IMSUT Hospital, Institute of Medical Science, University of Tokyo, Japan; and [5]Department of Microbiology and Immunology, Emory University School of Medicine, Atlanta, Georgia

The molecular mechanisms for *IL2* gene–specific dysregulation during chronic human immunodeficiency virus type 1 (HIV-1) infection are unknown. Here, we investigated the role of DNA methylation in suppressing interleukin 2 (IL-2) expression in memory CD4$^+$ T cells during chronic HIV-1 infection. We observed that CpG sites in the *IL2* promoter of CD4$^+$ T cells were fully methylated in naive CD4$^+$ T cells and significantly demethylated in the memory populations. Interestingly, we found that the memory cells that had a terminally differentiated phenotype and expressed CD57 had increased *IL2* promoter methylation relative to less differentiated memory cells in healthy individuals. Importantly, early effector memory subsets from HIV-1–infected subjects expressed high levels of CD57 and were highly methylated at the *IL2* locus. Furthermore, the increased CD57 expression on memory CD4$^+$ T cells was inversely correlated with IL-2 production. These data suggest that DNA methylation at the *IL2* locus in CD4$^+$ T cells is coupled to immunosenescence and plays a critical role in the broad dysfunction that occurs in polyclonal T cells during HIV-1 infection.

Keywords. HIV-1; CD4$^+$ T-cell dysfunction; repression of IL-2 expression; DNA methylation; T-cell differentiation; immunosenescence.

During chronic human immunodeficiency virus type 1 (HIV-1) infection, CD4$^+$ T cells undergo cell-intrinsic phenotypic and functional impairments that are coupled to increased pathogenesis. These phenotypic changes include elevated levels of expression of activation, exhaustion, and senescent markers [1–5]. We have previously reported reduction in the expression of specific cytokines by T cells in HIV-1 noncontrollers, which is associated with activation/exhaustion status in both CD4$^+$ and CD8$^+$ memory T cells [6]. It has also been observed that both HIV-1-specific CD4$^+$ and CD8$^+$ T cells are less functional, with a particular impairment in interleukin 2 (IL-2) transcriptional expression, in individuals with disease progression, compared with long-term nonprogressors [7–10]. These data suggest that loss of function in T cells is, in part, due to gene-specific transcriptional dysregulation that is acquired during chronic HIV-1 infection. However, molecular mechanisms underlying the gene-specific reduction in expression have not been elucidated.

Epigenetic mechanisms of transcriptional regulation are critical for tissue and gene-specific transcript expression. Recently, it has become clear that epigenetic marks, such as DNA methylation and chromatin modification, modulate helper T-cell lineage commitment and function [11–14]. Furthermore, detailed analysis of epigenetic modification at the PD-1 locus in both mouse and human T cells indicates that the DNA methylation program modulates memory T-cell quality during persistent viral infection [15, 16]. Additionally, DNA demethylation at the promoter/enhancer region near the transcriptional start site of several genes coding

Received 16 February 2014; accepted 25 June 2014.

Correspondence: Ai Kawana-Tachikawa, Division of Infectious Diseases, Advanced Clinical Research Center, Institute of Medical Science, University of Tokyo, 4-6-1 Shirokanedai, Minato-ku, Tokyo 108-8639, Japan (aikawana@ims.u-tokyo.ac.jp).

The Journal of Infectious Diseases

DOI: 10.1093/infdis/jiu376

for cytokines, including *IL2*, occurs after T-cell activation [17–19]. However, the role of epigenetic reprogramming of the *IL2* promoter in dysfunctional T cells during chronic HIV-1 infection has not been examined.

In the present study, we evaluated DNA methylation at the promoter/enhancer region of *IL2* in $CD4^+$ and $CD8^+$ T cells from HIV-1–infected noncontrollers with suppressed IL-2 expression. We also measured *IL2* promoter DNA methylation in T-cell subsets from HIV-1–uninfected donors to gain further insight into the link between changes in DNA methylation and downregulation of IL-2 expression. Finally, we investigated the relationship between *IL2* promoter DNA methylation and CD57, a marker of replicative senescence on T cells and a characteristic feature of T cells in HIV-1–infected individuals.

MATERIALS AND METHODS

Study Population

Peripheral blood mononuclear cells (PBMCs) were obtained from 16 viremic controllers (median HIV-1 RNA level, 410 copies/mL; interquartile range, 105–613 copies/mL) and 19 noncontrollers (median HIV-1 RNA level, 71 000 copies/mL; interquartile range, 60 500–86 000 copies/mL). Untreated chronic and viremic controller donors with $CD4^+$ T-cell counts of approximately 400 cells/μL were identified and used for this study, to ensure that differences in downstream assays were not due to reduction in $CD4^+$ T-cell quantity. Seven individuals in the acute stage of HIV-1 infection (defined as ≤3 months after diagnosis) were recruited. Individuals showing symptoms of acute HIV-1 infection had a dramatic decline in viral load, and 8 individuals received combination antiretroviral therapy (cART) for prolonged period and were also included in this study (Table 1). Eleven HIV-1–seronegative individuals were enrolled in this study. All participants gave written informed consent. The study was approved by the institutional review boards of the Institute of Medical Science at the University of Tokyo (20-47-210521).

Cell Culture and T-Cell Stimulation

The frozen PBMCs were thawed and rested overnight before use in Roswell Park Memorial Institute 1640 medium supplemented with 10% heat-inactivated fetal calf serum. The PBMCs were stimulated with 2 μg/mL phytohemagglutinin–L (Roche) for 2.5 or 5 hours. Total messenger RNA (mRNA) was extracted 2.5 hours after stimulation for quantification of cytokine gene expression. Culture supernatants were harvested after 5 hours of stimulation for measurement of cytokine production. The human cytokine 25-plex antibody kit (Invitrogen) was used for measurement of the concentrations of multiple cytokines in the supernatant [6].

Quantification of mRNA by Real-Time Polymerase Chain Reaction (PCR)

Total RNA was extracted from the stimulated PBMCs, using an RNeasy Mini Kit (Qiagen), and was reverse transcribed with SuperScript III reverse transcriptase (Invitrogen), according to the manufacturer's protocol, with oligo dT primers. Quantitative reverse-transcription PCR was performed with the LightCycler TaqMan Master Kit and the LightCycler 2.0 capillary-based system, using the Universal ProbeLibrary (Roche). All samples were run in duplicate. The gene encoding succinate dehydrogenase complex subunit A (*SDHA*) was used as a reference gene [20].

$CD4^+$ and $CD8^+$ T-Cell Isolation

$CD4^+$ and $CD8^+$ T cells were isolated from PBMCs by magnetic cell separation–positive selection, using anti CD4 and CD8 antibody-conjugated beads (Miltenyi Biotic), according to the

Table 1. Characteristics of Study Subjects, by Group

	Controller (n = 16)	Noncontroller (n = 19)	Acutely Infected (n = 7)	cART Recipient (n = 8)	HIV-1-uninfected (n = 11)	P^a
Viral load, HIV-1 RNA copies/mL	410 (105–613)	71 000 (60 500–86 000)	230 000 (156 000–715 000)	Undetectable[b]	. . .	<.0001
T-cell count, cells/μL						
$CD4^+$	401 (377–468)	417 (329–442)	418 (300–492)	742 (606–795)	. . .	NS
$CD8^+$	893 (695–1103)	1302 (837–1760)	1262 (810–1668)	981 (809–1173)	. . .	.025
Age, y	34 (27–47)	39 (35–46)	41 (36–46)	44 (40–50)	38 (34–42)	NS
Duration after diagnosis, mo	50 (20–78)	29 (18–39)	≤3	82 (63–93)	. . .	NS
Treatment duration, mo	NA	NA	NA	60 (38–70)	. . .	. . .

Data are median (interquartile range).

Abbreviations: cART, combination antiretroviral therapy; HIV-1, human immunodeficiency virus type 1; NA, not applicable; NS, not significant.

[a] Data denote results of comparisons between controllers vs noncontrollers.

[b] Lower limit of detection (50 copies/mL), except a patient with 80 copies/mL.

manufacturer's instructions. The purity of each cell fraction was >95%, as determined by flow cytometry.

DNA Methylation Analysis

The analysis of DNA methylation was determined by bisulfate sequencing as previously described [21]. Briefly, genomic DNA from the purified $CD4^+$ T cells and $CD8^+$ T cells were treated with bisulfate, using the EpiTect Bisulfite Kit (Qiagen). Converted DNA (50 ng) was amplified by PCR with AccuPrime Taq DNA polymerase. The PCR was performed with the following locus-specific primers: 5′-GAGATAGGATTTTTTTAAGTGTTTTTAGGT-3′ and 5′-CATTAACCCACACTTAAATAATAACTCTAA-3′ for the *IL2* gene, 5′-GTTAAGAGGGAGAGAAGTAATTATAGATTT-3′ and 5′-AAATCTATAATTACTTCTCTCCCTCTTAAC-3′ for the tumor necrosis factor gene (*TNF*), and 5′-TGGAAAGAGGAGAGTGACAGAA-3′ and 5′-TTGGATGCTCTGGTCATCTTTA-3′ for the interferon γ gene (*IFNG*). The PCR products were cloned into the pGEM-T Easy vector system (Promega), and sequencing analysis was performed with at least 10 individual clones from each sample. All independent experiments were duplicated to avoid PCR amplification bias.

Antibodies

The following antibodies were used for flow cytometric analysis and cell sorting: CD57–fluorescein isothiocyanate (FITC), PD1-FITC, IL2-FITC, CD28–allophycocyanin (APC), CD45RA-APC, CCR7-phycoerythrin (PE)-Cy7, and CD3–Pacific blue (BD Pharmingen); CD27-FITC, CD8-PE, and CD3-peridinin chlorophyll protein-Cy5.5 (BD Biosciences); CD57-PE, CD45RA-APC-Cy7, CD4–Pacific blue, and CD8–Pacific blue (BioLegend); and CD4-APC-eFluor780 (eBioscience). Dead or dying cells were detected by staining with propidium iodide (Sigma).

Flow Cytometric Analysis and Cell Sorting of $CD4^+$ T-Cell Subsets

Multiparameter flow cytometry and cell sorting were performed with an Aria fluorescence-activated cell sorter (BD). Intracellular cytokine staining and surface staining were preformed as previously described [6]. For cell sorting, the sort logic was set by gating lymphocytes by forward scatter and side scatter and then gating on $CD3^+CD4^+$ cells. For methylation analysis of $CD4^+$ T-cell subsets, $CD4^+$ T cells were classified into 5 subsets based on expression of CD45RA, CCR7, CD27, and CD28: $CD45RA^+CCR7^+CD27^+CD28^+$ (naive), $CD45RA^-CCR7^+CD27^+CD28^+$ (central memory), $CD45RA^{+/-}CCR7^-CD27^+CD28^+$ (early effector memory), $CD45RA^{+/-}CCR7^-CD27^-CD28^+$ (intermediate effector memory), and $CD45RA^{+/-}CCR7^-CD27^-CD28^-$ (late effector memory). Memory $CD4^+$ T cells ($CD3^+CD4^+CD45RA^-$) were classified into further subsets based on expression of CD57. The purity of the sorted cell populations was >99%.

Statistical Analysis

GraphPad Prism5 software (GraphPad Software) was used for all statistical analysis. The Mann–Whitney *U* test and the Wilcoxon matched paired test were used for unpaired and paired comparisons, respectively. Correlation analysis was performed using Spearman rank correlation. Correction for multiple comparisons was assessed by calculating *q* values, the *P* value analogue of the false-discovery rate [22]. The level of significance for all analyses was set at a *P* value of <.05 and a *q* value of <0.2.

RESULTS

IL2 Gene Expression Is Impaired in HIV-1–Infected Noncontrollers During Chronic Infection

To elucidate a qualitative difference between T cells from viremic controllers and those from noncontrollers during chronic HIV-1 infection, we broadly assayed cytokine expression profiles from phytohemagglutinin-L (PHA)-stimulated PBMCs isolated from individuals with chronic HIV-1 infection. We found that IL-2, tumor necrosis factor α, interleukin 6, and interleukin 7 expression was significantly impaired in noncontrollers (Figure 1*A*). Because *IL2*, *TNF*, and *IL6* are early response genes that trigger sequential multiple immune responses and share some signaling pathways, we further examined mRNA expression of these genes at an earlier time point after PHA stimulation, to determine the hierarchy of reexpression. Importantly, the level of *IL2* mRNA expression was almost 4-fold higher in controllers relative to noncontrollers, whereas *TNF* and *IL6* mRNA expression levels were similar (Figure 1*B*). Furthermore, impaired *IL2* mRNA expression in noncontroller PBMCs was also observed after anti-CD3/CD28 stimulation (Supplementary Figure 1*A*). These data suggest that $CD4^+$ T cells in noncontrollers were qualitatively distinct in *IL2* gene regulation.

The *IL2* Promoter/Enhancer Region Is Hypermethylated in HIV-1–Infected Noncontrollers

Epigenetic modifications are a critical mechanism for stable gene expression. Specifically, acquired DNA methylation–mediated gene silencing can be maintained in a dividing population of cells [23–26]. The human *IL2* promoter contains 6 CpG sites within 1 kb immediately upstream of the transcriptional start site (Figure 2*A*) [18]. To investigate the role of DNA methylation in the restricted *IL2* expression in noncontrollers, we performed bisulfate sequencing to assess the level of DNA methylation at the individual CpG sites of the *IL2* promoter in $CD4^+$ and $CD8^+$ T cells isolated from HIV-1–infected individuals. The methylation frequency at all CpG sites in $CD4^+$ T cells was significantly higher in noncontrollers relative to that for $CD4^+$ T cells from controllers and HIV-1-uninfected individuals (Figure 2*B* and 2*C*). Notably, the difference was prominent in CpG site 1. In contrast, there was no significant

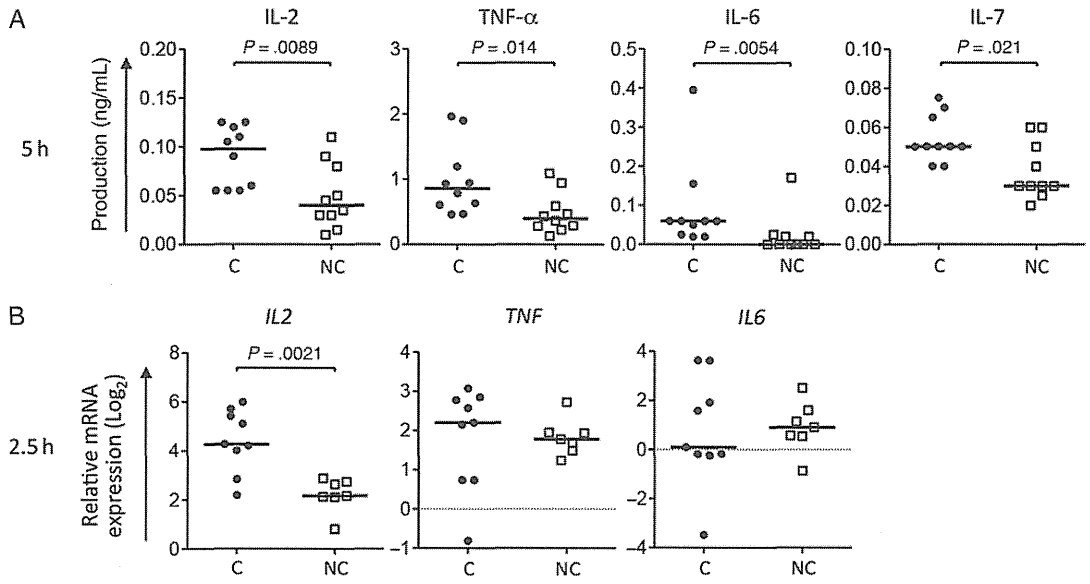

Figure 1. Cytokine transcription and protein expression profiling of phytohemagglutinin L (PHA)–stimulated peripheral blood mononuclear cells from individuals with chronic human immunodeficiency virus type 1 infection. Cytokine production (*A*) and messenger RNA (mRNA) expression of cytokines (*B*) after PHA stimulation. Data are normalized to the reference gene *SDHA* and are presented as fold change relative to unstimulated conditions. The horizontal bars indicate the median value. The Mann–Whitney *U* test was used for statistical analysis. Abbreviations: C, viremic controller; NC, noncontroller; IL-2, interleukin 2; IL-6, interleukin 6; IL-7, interleukin 7; TNF-α, tumor necrosis factor α.

difference in the methylation status of the *IL2* promoter in $CD8^+$ T cells between the groups (Figure 2*B* and Supplementary Figure 2*A*). It has previously been reported that *IFNG* and *TNF* promoters undergo methylation in aged people [27, 28]. Therefore, we sought to determine whether these promoters also acquired methylate promoters during chronic HIV-1 infection. Our bisulfite sequencing data indicate that there is not a significant difference in DNA methylation of the both *IFNG* and *TNF* promoter in $CD4^+$ and $CD8^+$ T cells between HIV-1 controllers and noncontrollers (Supplementary Figure 2*B* and 2*C*). To further determine whether the increase in methylation of the *IL2* promoter was coupled to a reduction in expression, we measured IL-2 expression in PHA-stimulated PBMCs and compared it to the *IL2* promoter methylation status in $CD4^+$ T cells. The DNA methylation status at CpG site 1 in $CD4^+$ T cells was inversely correlated to *IL2* mRNA expression and IL-2 production (Figure 2*D*). The inverse correlation was also observed when anti-CD3/CD28 was used as a stimulus (Supplementary Figure 1*B*). These data indicate that DNA hypermethylation at CpG site 1 in $CD4^+$ T cells is coupled to low IL-2 expression in noncontrollers during chronic HIV-1 infection.

$CD4^+$ T Cells From cART Recipients Have a Hypomethylated *IL2* Promoter

We next examined the DNA methylation status of the *IL2* promoter in $CD4^+$ T cells at different clinical stages of HIV-1 infection. We measured the methylation status of the *IL2* promoter in $CD4^+$ T cells from HIV-1–infected individuals with a high viral load in the acute stage of infection (Figure 2*E*). Surprisingly, the level of methylation of the *IL2* promoter in $CD4^+$ T cells from HIV-1–infected individuals in the acute stage of infection was similar to $CD4^+$ T cells from controllers and those from HIV-1-uninfected individuals. These data suggest that a high viral load itself does not affect the methylation status of the *IL2* locus.

We next sought to determine whether reduction of the HIV level in chronically infected individuals would result in demethylation of the *IL2* promoter. We performed a longitudinal analysis of *IL2* promoter methylation in $CD4^+$ T cells isolated from individuals before they received cART and after they achieved prolonged cART-mediated virus suppression. The subjects with prolonged viral suppression had recovery in $CD4^+$ T-cell counts, and, importantly, hypermethylation at CpG site 1 in the *IL2* locus before starting cART declined to normal levels after prolonged virus suppression in all individuals (Figure 2*F*). Indeed, the level of *IL2* promoter methylation in treated individuals was similar to the promoter methylation levels in HIV-1 controllers and uninfected individuals (Figure 2*E*). These data suggest that *IL2* promoter hypermethylation results from persistent high viral loads but is reversible after cART-mediated virus suppression.

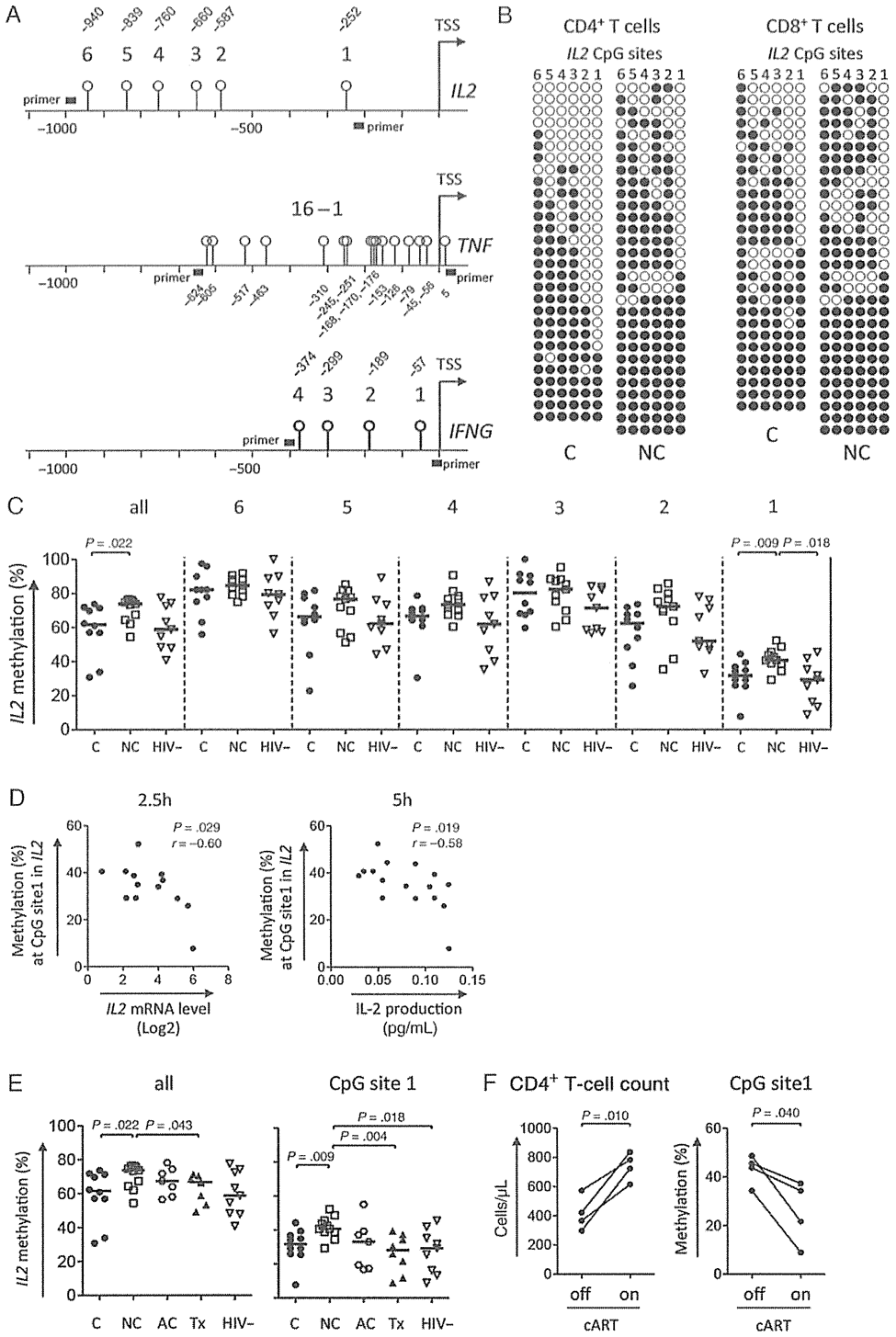

Figure 2. DNA methylation analysis of the *IL2* locus in human immunodeficiency virus type 1 (HIV-1)–infected individuals. *A*, Diagram of CpG position relative to the transcriptional start site of the *IL2, TNF,* and *IFNG* loci. *B*, Representative bisulfite sequencing DNA methylation analysis of the *IL2* locus in $CD4^+$ and $CD8^+$ T cells from viremic controllers and noncontrollers. Each line represents an individual clone picked for sequencing (filled circles, methylated cytosine; open circles, unmethylated cytosine). *C*, DNA methylation status of the *IL2* locus at CpG sites 1–6 in $CD4^+$ T cells from healthy and HIV-1–infected individuals. *D*, Correlation plot between methylation at CpG site 1 in $CD4^+$ T cells and interleukin 2 (IL-2) expression in peripheral blood mononuclear cells. *E*, DNA methylation status in all and at CpG site 1 in $CD4^+$ T cells at different clinical status in HIV-1 infection. *F*, Longitudinal change of methylation status at CpG site 1 and $CD4^+$ T-cell count in 4 subjects before and after combination antiretroviral therapy initiation. The Mann–Whitney *U* test (*C* and *E*) and the Wilcoxon matched paired test (*F*) were used for statistical analysis. Correlation coefficient and *P* values determined by the Spearman rank correlation test are shown in panel *D*. Abbreviations: AC, acute HIV-1 infection; C; controller, NC; noncontroller; Tx, treated with combination antiretroviral therapy; HIV-, HIV-1-uninfected.

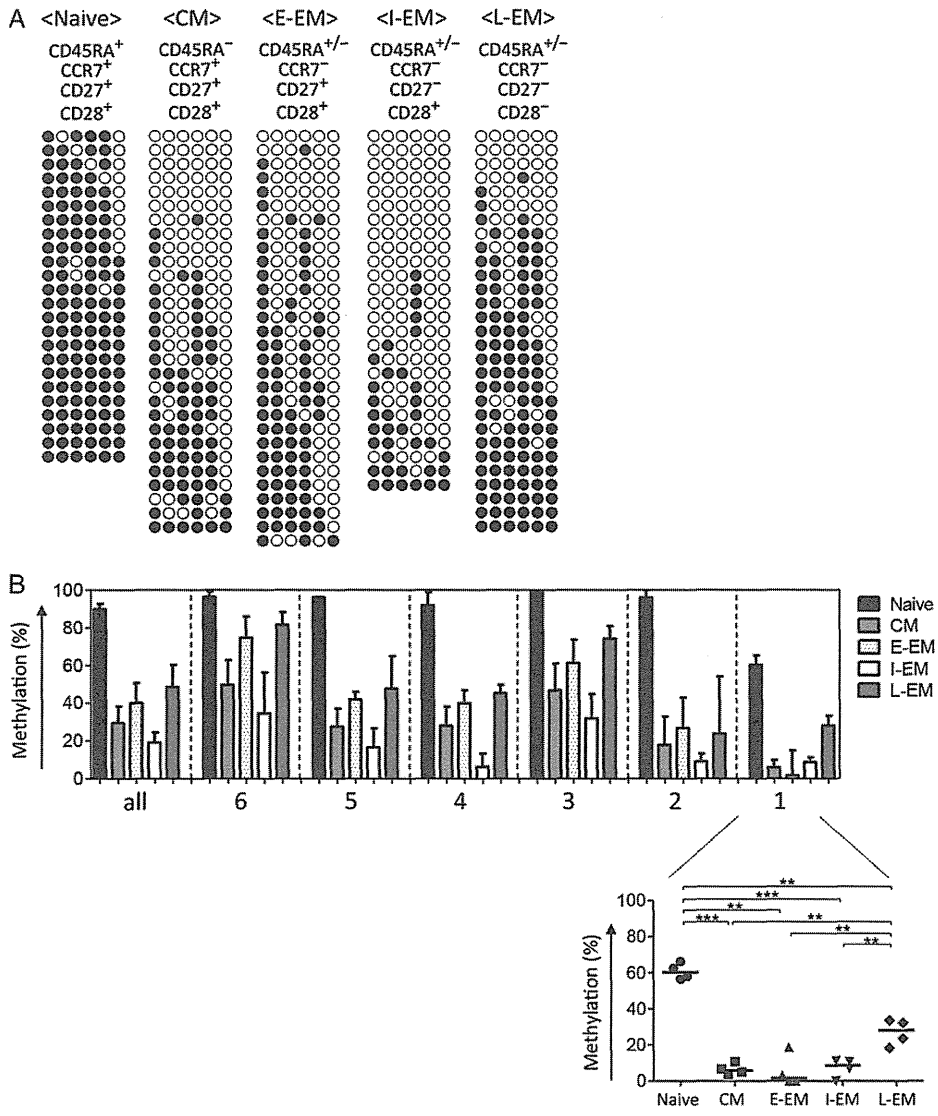

Figure 3. DNA methylation status of the *IL2* locus in different CD4+ T-cell subsets. *A*, Representative bisulfite sequencing DNA methylation analysis of the *IL2* locus in naive, central memory (CM), early effector memory (E-EM), intermediate effector memory (I-EM), and late effector memory (L-EM) CD4+ T-cell subsets, classified according to CD45RA, CCR7, CD27, and CD28 expression. *B*, Summary graph of DNA methylation status of the *IL2* locus in T-cell subsets in 4 individuals without HIV-1 infection. The paired *t* test was performed for statistical analysis. $^{**}P = .001–.01$, $^{***}P < .001$.

Phenotypically Senescent Memory CD4+ T Cells Have a Methylated *IL2* Promoter

Although the DNA methylation status of the *IL2* promoter/enhancer region in different CD4+ T cells in mice has been well characterized [17, 29, 30], the detailed profile of *IL2* promoter methylation in human CD4+ T cells has not been elucidated. Therefore, we sorted different CD4+ T-cell subsets in HIV-1-uninfected individuals on the basis of CD45RA, CCR7, CD27, and CD28 expression [31–33] and assessed the methylation status of the *IL2* promoter in each fraction (Figure 3). CpG sites 2–6 were fully methylated, and CpG site 1 was 60% methylated in naive CD4+ T cells (Figure 3*A* and 3*B*). In contrast, CpG sites 2–6 were >50% demethylated in all memory subsets (Figure 3*B*). Moreover, CpG site 1 was fully demethylated in central memory, early effector memory, and intermediate effector memory cell compartments (Figure 3*B*). Interestingly, all CpG sites, including site 1, were remethylated in late effector memory cells. Since signaling through CD28 has been shown to modify the epigenetic program of the *IL2* promoter in mice [30], we postulated that the *IL2* promoter may have an altered DNA methylation program in late effector memory subsets without CD28 expression.

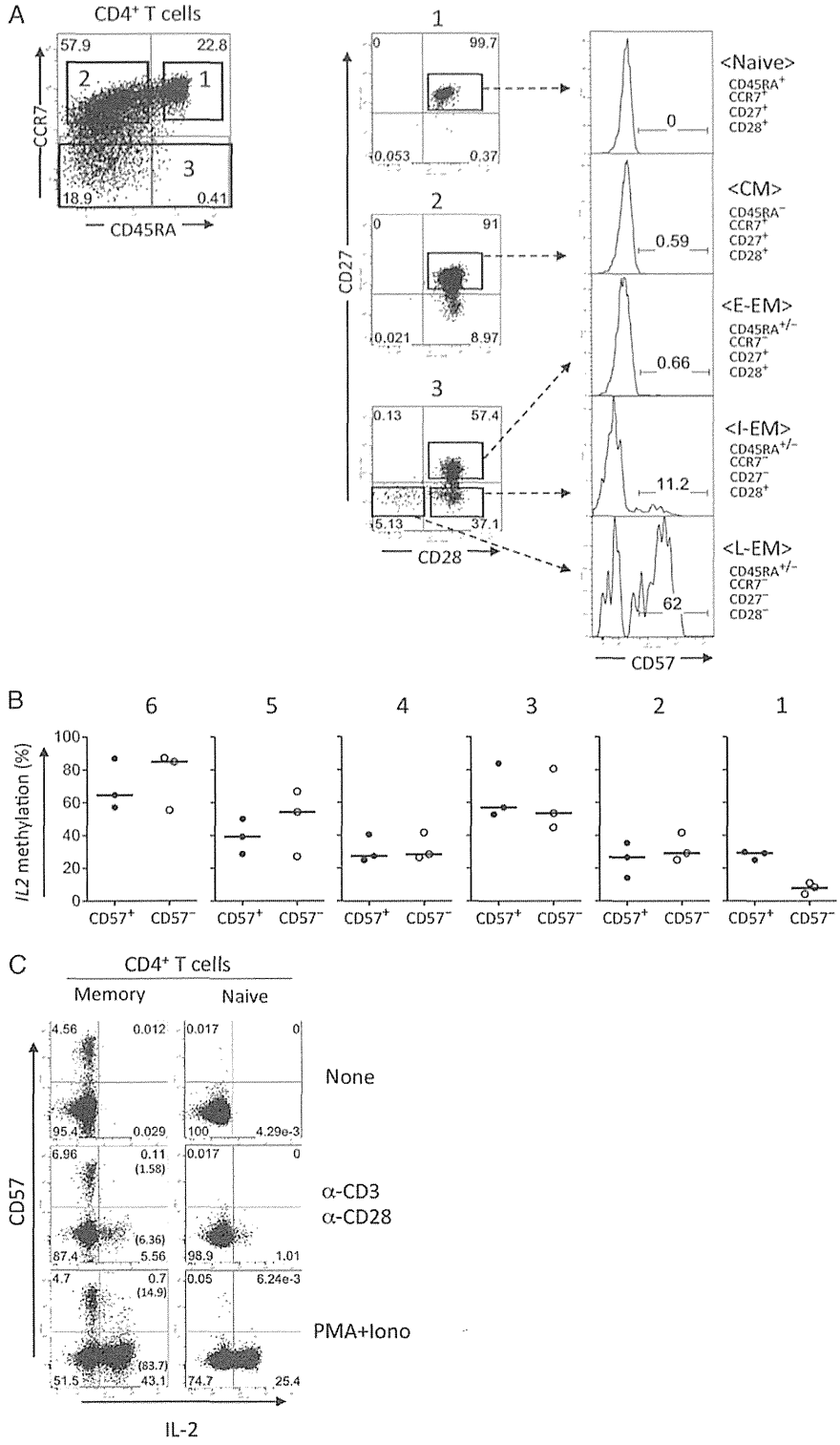

Figure 4. Analysis of CD57 expression and *IL2* locus DNA methylation in memory CD4+ T-cell subsets. *A*, Representative flow cytometric analysis of CD57 expression on CD4+ T-cell subsets classified by CD45RA, CCR7, CD27, and CD28 expression. *B*, Summary graph of the *IL2* locus DNA methylation status at CpG sites 1–6 in CD57+ and CD57− memory (CD45RA−) CD4+ T cells from 3 individuals without human immunodeficiency virus type 1 (HIV-1) infection. *C*, Flow cytometric analysis of CD57 and IL-2 expression after stimulation with α-CD3/CD28 and PMA/ionomycin in peripheral blood mononuclear cells from an HIV-1-uninfected individual. Values within brackets indicate the proportion of IL-2 secreting cells in CD57+ and CD57− cells. Abbreviations: CM, central memory; E-EM, early effector memory; I-EM, intermediate effector memory; L-EM, late effector memory.

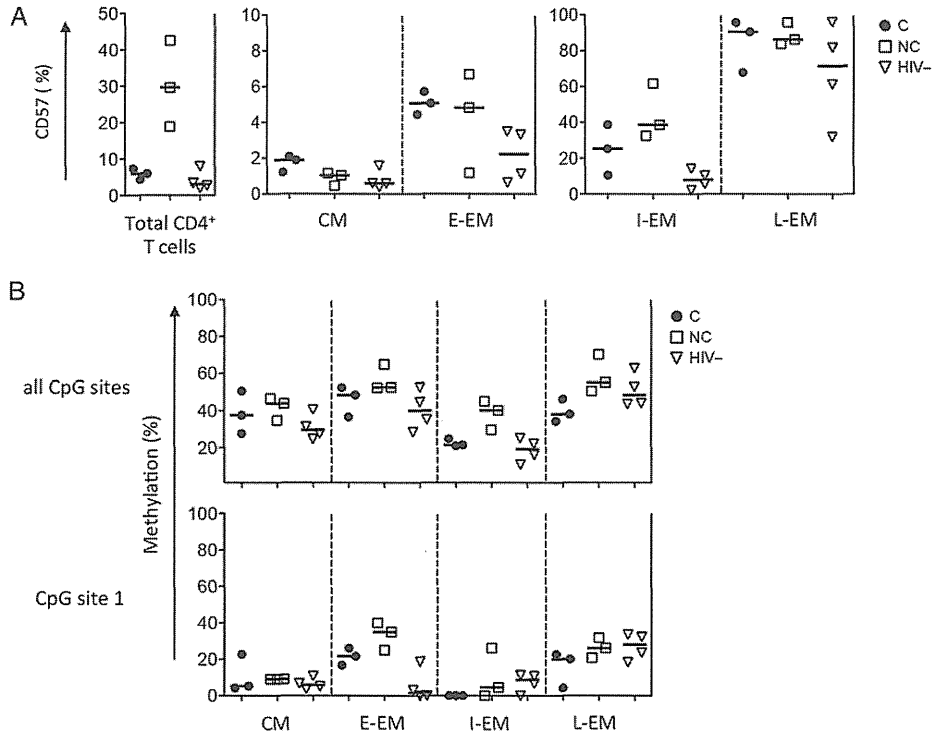

Figure 5. DNA methylation analysis of the *IL2* locus in memory $CD4^+$ T-cell subsets from individuals with chronic human immunodeficiency virus type 1 (HIV-1) infection. Summary graphs of CD57 expression level (*A*) and DNA methylation status of the *IL2* locus (*B*) in memory $CD4^+$ T-cell subsets. The memory subsets were defined by CD45RA, CCR7, CD27, and CD28 expression as shown in Figure 4*A*. Abbreviations: C, viremic controller; NC, noncontroller; HIV-, HIV-1-uninfected; CM, central memory; E-EM, early effector memory; I-EM, intermediate effector memory; L-EM, late effector memory.

It has also been reported that expression of CD57 is highly correlated with loss of CD28 expression in $CD4^+$ T cells [34–36] and is associated with replicative senescent T cells [34, 37, 38]. On the basis of these observations, we evaluated the association between CD57 expression and DNA methylation of the *IL2* promoter. We first analyzed CD57 expression in each $CD4^+$ T-cell subset. Naive, central memory, and early effector memory $CD4^+$ T cells from healthy individuals did not express CD57, while a significantly increased frequency of $CD4^+$ T-cell subsets with a more differentiated phenotype expressed CD57, with the highest level of expression observed on the late effector memory subset. We next assessed the DNA methylation status of the *IL2* promoter in $CD57^+$ and $CD57^-$ subsets of memory ($CD45RA^-$) $CD4^+$ T cells (Figure 4*B*). We found that CpG site 1 was more methylated in the $CD57^+$ subsets relative to the $CD57^-$ subsets. Importantly, IL-2 secretion in CD57-expressing memory $CD4^+$ T cells was 5-fold lower than IL-2 secretion in $CD57^-$ memory $CD4^+$ T cells even after strong T-cell stimulation with PMA/ionomycin (14.9% vs 83.7%; Figure 4*C*). These data indicate that $CD57^+$ cells among late effector memory $CD4^+$ T cells were remethylated at CpG site 1 of the *IL2* promoter, which was coupled to restricted IL-2 expression.

$CD57^+CD4^+$ T Cells in HIV-1–Infected Noncontrollers Have a Methylated *IL2* Promoter and Restricted IL-2 Expression

It has also been reported that HIV-1-specific $CD57^+CD4^+$ T cells have reduced IL-2 expression [35, 39]. Abnormal T-cell differentiation of polyclonal $CD4^+$ and $CD8^+$ T cells in HIV-1-infected individuals is associated with increased levels of CD57 expression [5, 35]. To determine whether the increased immune dysfunction in polyclonal memory T cells during chronic HIV-1 infection is associated with stable epigenetic programming of the memory pool, we measured DNA methylation of the *IL2* promoter in memory $CD4^+$ T-cell subsets from HIV-1–infected individuals. As previously reported [5, 35], the number of $CD57^+$ effector memory (early, intermediate, and late) $CD4^+$ T cells was higher in chronically infected individuals, compared with individuals without HIV infection (Figure 5*A*). We also observed an increase in methylation of the *IL2* promoter, not only in the late effector memory subset, but also in the less differentiated early effector memory and intermediate effector memory subsets from noncontrollers (Figure 5*B*). These data suggest that aberrant epigenetic modification at *IL2* promoter, coupled to CD57 expression, occurs at an early stage of $CD4^+$ T-cell differentiation during chronic HIV-1 infection.